1. Report No.	2. Government Accession No	3. Recipient's Catalog No.
[*UT-23-RP-01*]	N/A	N/A

4. Title and Subtitle	5. Report Date
Thermally Conductive Pre-cast Concrete Pavement for Urban Heat Island mitigation	***[December 1st, 2025]***
	6. Performing Organization Code N/A

7. Author(s)	8. Performing Organization Report No.
Islam Radwan, MSc, ORCID: https://orcid.org/0009-0008-2767-8563 Samer Dessouky, PhD, PE, ORCID: https://orcid.org/0000-0002-6799-6805 Hatim Sharif, PhD, PE, ORCID: https://orcid.org/0000-0001-9805-8080	**[*UT-23-RP-01*]**

9. Performing Organization Name and Address	10. Work Unit No.
University of Texas at San Antonio (UTSA) School of Civil & Environmental Engineering, and Construction Management 1 UTSA Circle, San Antonio, TX 78249	N/A
	11. Contract or Grant No. 69A3552348333

12. Sponsoring Organization Name and Address	13. Type of Report and Period Covered
• Transportation Infrastructure Precast Innovation Center (TRANS-IPIC) University of Illinois Urbana-Champaign 205 N Mathews Ave, Urbana, IL 61801 • US Department of Transportation, Office of Research, Development and University of Technology (RD&T), 1200 New Jersey Avenue, SE, Washington, DC 201590	Final Report, September 2023-December 2025
	14. Sponsoring Agency Code N/A

15. Supplementary Notes
For additional reports and information visit the TRANS-IPIC website https://trans-ipic.illinois.edu

16. Abstract
Urban areas experience elevated pavement temperatures due to the urban heat island (UHI) effect, which increases cooling energy demand and associated carbon emissions. In this project, the work focused on three main components: (1) a comprehensive mechanical study of precast concrete mixes containing microencapsulated organic phase change material (PCM), (2) three-dimensional transient thermal finite element (FE) simulations, and (3) full-scale sidewalk testing evaluated using a Monthly Cooling Benefit Index (MCBI). The mechanical program quantified the influence of PCM dosage on workability and compressive strength and showed a clear trend of decreasing strength with increasing PCM content. However, mixes with moderate PCM dosages retained adequate strength for sidewalk applications, while still providing measurable cooling potential. The calibrated 3D FE model captured the main experimental trends by representing PCM as an increase in effective heat capacity and a reduction in thermal diffusivity. Simulation results confirmed that PCM integration consistently reduced peak surface temperatures relative to the control slab, with mid-range PCM contents offering the best balance between thermal moderation and mechanical performance. A full-scale pilot sidewalk with multiple precast segments—combining PCM with different surface finishes such as sandblasting and diamond grinding—was constructed on the University of Texas at San Antonio campus and monitored over continuous three months. Field measurements showed that segments with moderate PCM content (e.g., around 2.5%) coupled with reflective/high-albedo surface treatments achieved the most persistent reductions in surface temperature compared with the conventional control and PCM-only panels. When quantified using the MCBI, the sandblasted and diamond-ground PCM segments ranked highest, indicating that the combined strategy of moderate PCM dosage and optimized surface finishing provides the most effective and practical cooling benefit for UHI mitigation in urban sidewalks.

17. Key Words	18. Distribution Statement
Urban Heat islands; Sidewalks; Cool pavements; Phase change materials; Thermal energy storage; Sustainable transportation infrastructure	No restrictions.

19. Security Classification (of this report)	20. Security Classification (of this page)	21. No. of Pages	22. Price
Unclassified.	Unclassified.	55	N/A

Disclaimer:

The contents of this report reflect the views of the authors, who are responsible for the facts and the accuracy of the information presented herein. This document is disseminated in the interest of information exchange. The report is funded, partially or entirely, under 69A3552348333 from the U.S. Department of Transportation's University Transportation Centers Program. The U.S. Government assumes no liability for the contents or use thereof.

Transportation Infrastructure Precast Innovation Center (TRANS-IPIC)

University Transportation Center (UTC)

Thermally Conductive Pre-cast Concrete Pavement for Urban Heat Island mitigation

[*UT-23-RP-01*]

FINAL REPORT

Submitted by:
Islam Radwan, Graduate PhD Candidate, *Islam.Radwan@my.utsa.edu*
Samer Dessouky (PI), Professor, Samer.dessouky@utsa.edu
Hatim Sharif (CO-PI), Professor, hatim.sharif@utsa.edu
School of Civil & Environmental Engineering and Construction Management
University of Texas at San Antonio

Collaborators / Partners:
Microtek laboratories Company
City of San Antonio
Tindall Corporation

Submitted to:
TRANS-IPIC UTC
University of Illinois Urbana-Champaign
Urbana, IL

Executive Summary:

Urban areas experience elevated surface temperatures due to the Urban Heat Island (UHI) effect, which increases cooling loads, energy use, and heat-related health risks. Conventional concrete pavements store and reradiate solar energy, adding to this problem. This project advances a thermally adaptive precast concrete sidewalk system that incorporates microencapsulated organic phase change material (PCM) to passively reduce pavement surface temperatures and improve pedestrian thermal comfort. The work focused on three components: (1) a mechanical study of PCM-integrated precast mixes, (2) development and calibration of a three-dimensional transient finite element (FE) model for PCM concrete slabs, and (3) a full-scale pilot sidewalk test section on the UTSA campus evaluated using a Monthly Cooling Benefit Index (MCBI). PCM was incorporated by both an addition method (percentage of total mix weight) and a sand-replacement method (replacing part of the fine aggregate) at dosages up to 10%. Compressive strength and workability were measured at multiple ages to confirm suitability for precast sidewalk production. Strength decreased with increasing PCM, with the largest loss at 10%, but mixes with moderate contents especially the 5% PCM sand-replacement mix maintained acceptable strength and workability while benefiting from enhanced thermal storage and reduced thermal diffusivity. Thus, a 5% PCM sand-replacement dosage offers a practical balance between mechanical performance and cooling potential for sidewalk applications. A 3D transient FE model was developed in ABAQUS, representing PCM through increased effective heat capacity over its phase-change range and reduced thermal diffusivity. The model was calibrated using multi-hour heating–cooling cycles, including an 8-hour cycle (4 hr. heating plus 4 hr. cooling) for the addition-method slabs. For the control slab, the FE model reproduced measured top- and bottom-surface temperature histories with root-mean-square errors (RMSE) of about 1 °C, capturing the rise from roughly 30 °C to mid-60s °C and the through-thickness gradient. With 5% PCM (addition method), experiments showed a slower temperature rise and lower peak surface temperature; the FE model captured these trends with RMSE values around 1.5–1.6 °C during heating and slightly lower during cooling. Overall, the simulations confirmed that PCM integration delays heat penetration and moderates peak temperatures, and that moderate PCM contents provide the most efficient balance between cooling benefit and material performance when heating duration approaches the PCM latent-heat capacity. Full-scale precast sidewalk test section of six 4 ft × 4 ft slabs was constructed on the UTSA campus using only the sand-replacement method: a conventional control, a 5% PCM slab, a sandblasted high-albedo slab without PCM, a sandblasted slab with 2.5% PCM, a slab with diamond grinding without PCM, and a slab with diamond grinding with 2.5% PCM. Surface temperatures were monitored for about three months (July–September 2025) to capture summer diurnal cycles. The control slab exhibited the highest peaks; slabs with PCM only or surface treatment only showed intermediate cooling; and the combined strategies sandblasted plus 2.5% PCM and diamond grinding plus 2.5% PCM consistently produced the lowest peak temperatures and most persistent reductions during the hottest hours. An MCBI was formulated from the monitored temperatures to represent cumulative cooling over representative summer months. Ranked by MCBI, the combined systems with 2.5% PCM plus sandblasting or diamond grinding achieved the highest cooling benefit, followed by the PCM-only and surface-treatment-only slabs, with the control lowest. Taken together, the mechanical results, FE modeling, and full-scale monitoring show that PCM-enhanced precast concrete optimized around a 5% PCM sand-replacement mix for structural adequacy and deployed in the field using 2.5% PCM with reflective surface finishes offers a practical, scalable strategy for mitigating UHI effects in urban sidewalks and provides an engineering-based framework for design and implementation.

Table of Contents

List of Tables

Problem Statement:

Rapid urbanization has increased the fraction of impervious, heat-absorbing surfaces in cities, leading to the well-documented (UHI) effect, where urban areas experience higher air and surface temperatures than their surrounding rural regions. Paved surfaces including streets, parking lots, and sidewalks account for a large share of urban land covering and store substantial amounts of solar energy during the day, which is then released as sensible heat into the urban canopy layer. This process elevates near-surface air temperatures, increases building cooling demand, worsens air quality and ozone formation, and exacerbates heat-related health risks, particularly for pedestrians and transit users who spend extended periods near pavement surfaces. Conventional concrete pavements contribute to UHI because of their relatively high thermal conductivity, moderate to low albedo, and high heat storage capacity. Once heated, these pavements cool slowly, maintaining elevated surface temperatures into the evening and nighttime. In dense urban environments, this stored heat interacts with building envelopes and surrounding infrastructure, reinforcing the local energy imbalance, and increasing the carbon footprint associated with space cooling and peak electricity demand. Existing mitigation strategies—such as high-albedo "cool" coatings, permeable pavements, and urban greening—can reduce surface temperatures but face several limitations: coatings may degrade under traffic and environmental wear, permeable systems may not be suitable for all soils or maintenance regimes, and vegetation-based solutions are constrained by available space, water demand, and long establishment periods. Sidewalks are a critical but often under-addressed component of this problem. They are in direct, frequent contact with pedestrians, bicyclists, and transit riders, and elevated sidewalk surface temperatures directly affect pedestrians' thermal comfort and safety, especially during extreme heat events. At the same time, municipal agencies must satisfy practical constraints related to constructability, cost, durability, and compatibility with existing standards and contracting practices. There is a pressing need for cool pavement technologies that can be implemented using familiar materials and construction methods, while providing measurable and durable reductions in surface temperature. One promising approach is to develop thermally adaptive concrete pavements by incorporating microencapsulated phase change materials (PCM) within the concrete matrix. PCMs can absorb and release large amounts of latent heat near their phase-transition temperature, effectively buffering temperature swings and reducing peak surface temperatures without relying on external energy inputs. In this project, an experimental program was carried out on precast concrete slabs with PCM incorporated using both an addition method and a sand-replacement method at different dosages (Radwan & Dessouky, 2024). (Radwan & Dessouky, 2024) quantified the effects of PCM on thermal properties (heat capacity, thermal conductivity, and diffusivity) and demonstrated, through controlled indoor and outdoor heating–cooling cycles, that PCM-enhanced concrete can meaningfully reduce peak surface temperatures compared with conventional mixes. However, initial findings also highlighted important remaining questions: the need to systematically evaluate the mechanical performance of PCM-integrated mixes suitable for transportation infrastructure, to develop and validate numerical models capable of predicting PCM concrete behavior under realistic boundary conditions, and to confirm long-term cooling benefits and constructability through full-scale field installations. This report addresses these gaps by expanding the investigation in three directions: (1) conducting a comprehensive mechanical study of PCM-integrated precast concrete mixes, with particular emphasis on the sand-replacement method; (2) developing and calibrating a three-dimensional finite element thermal model for PCM concrete slabs; and (3) implementing and monitoring a full-scale precast sidewalk pilot on the UTSA

campus evaluated through a MCBI. By building directly on the thermal insights from the lab experiments published by (Radwan & Dessouky, 2024) and extending the work to structural performance, numerical modeling, and field validation, the project advances PCM-enhanced precast sidewalks as a practical, agency-ready strategy to improve pedestrian thermal comfort and mitigate UHI within existing transportation infrastructure programs.

CHAPTER 1: INTRODUCTION

BACKGROUND

In urban settings, cities experience a temperature rise of several degrees compared to rural and suburban regions, a phenomenon known as the (UHI) effect. This thermal disparity is attributed to the interplay between the built environment and human activities, with distinct heat balances evident in building materials versus natural surfaces [1], [2], [3]. Concrete, due to its substantial thermal inertia and dark color, is particularly prone to absorbing and retaining solar radiation [4], [5], [6], [7]. This solar absorption predominantly converts into sensible heat, as the impervious nature of pavements limits evaporative cooling [6], [7], [8]. The released sensible heat elevates urban air temperatures, contributing to the UHI phenomenon. Given that pavements cover 20–40% of a typical city's surface [9], [10], the concept of cool pavements has emerged as a potential solution to combat UHI. The "heat island effect" describes the higher temperatures found in the atmosphere and surfaces within urbanized areas compared to adjacent nonurbanized regions, typically underdeveloped or rural [11]. In cities with populations exceeding 1 million, the average annual air temperature is 1.8–5.4°F (1–3°C) higher than in neighboring areas [12]. Notably, during clear and calm summer nights, this temperature difference can soar to as much as 22°F (12°C) [13]. The UHI effect exemplifies inadvertent climate modification due to urbanization's impact on Earth's surface and atmospheric properties. Beyond the city-wide temperature impact, "heat island" also refers to localized effects at specific sites, where developed areas show higher temperatures than their immediate surroundings. Examples include buildings, parking lots, or airports adjacent to open spaces with bare soil or vegetation, creating localized hot spots in the urban landscape.

Cool pavements can be realized through various approaches, such as altering existing pavement materials, employing innovative designs, or introducing new materials into traditional pavements [14]. These pavements maintain lower temperatures by enhancing solar reflectance, promoting evaporation, and reducing sensible heat released into the urban environment. These cooling strategies are categorized as reflective pavements, evaporative pavements, and heat-harnessing pavements. Reflective pavements, with higher albedo, reduce surface temperatures by reflecting more sunlight and releasing less sensible heat [14], [15]. Evaporative pavements lower temperatures by retaining water on their surface or lower layers for cooling through evaporation [15]. Conversely, heat-harnessing pavements reduce surface temperatures by utilizing absorbed heat as renewable energy for other purposes [15], [16]. The discussion on cool pavements also considers their impact on urban climates, exploring the benefits, drawbacks, costs, and policies associated with these technologies [15], [16], [17]. The recent introduction of PCMs aims to improve the thermal properties of construction materials [16]. These materials can store and release significant thermal energy during phase transitions. PCMs, classified into organic, inorganic, and eutectic types, have been integrated into materials like concrete and gypsum, significantly enhancing their thermal mass. This enhancement plays a key role in moderating indoor temperatures and conserving energy in buildings. Additionally, PCMs may improve mechanical

and durability aspects of construction materials [16]. For instance, studies have examined their ability to regulate temperature fluctuations and heat generation during concrete hydration, improve crack resistance, and reduce thermal shrinkage. Researchers have also explored their potential to minimize thermal stress and damage in concrete pavements exposed to freeze-thaw cycles or temperature gradients. However, integrating PCMs into construction materials, particularly concrete, presents challenges [16]. Concerns have arisen about potential PCM leakage in their liquid state, which could interfere with cement hydration and negatively impact concrete's mechanical properties. Various methods have been proposed to safely integrate PCMs into construction materials, preventing leakage when in a molten state [16]. These methods, categorized as microencapsulation, shape-stabilized phase change materials (SSPCMs), porous aggregate inclusions, and macro-encapsulation, must be carefully considered for their specific applications and their effects on the host material's characteristics. PCMs absorb excess heat during high temperatures and release it when temperatures drop, reducing thermal gradients and the associated risk of cracking [18]. Studies have demonstrated significant reductions in peak temperatures and delays in reaching maximum temperatures when PCMs are incorporated into concrete, helping to manage the heat generated during cement hydration [19]. In colder climates, PCMs reduce the frequency of freeze/thaw cycles, thereby mitigating damage from ice formation within the concrete matrix [20]. Incorporating PCMs into concrete pavements presents a promising method to improve pavement thermal performance, particularly for mitigating ice and snow accumulation issues. PCMs can absorb, store, and release thermal energy during phase transitions, helping maintain pavement surfaces above freezing temperatures, which reduces the need for deicing chemicals and mechanical snow removal [21], [22]. Several methods have been developed to integrate PCMs into concrete pavements. One effective approach is using lightweight aggregates (LWA) impregnated with PCM. These aggregates are mixed into concrete, providing uniform PCM distribution throughout the pavement structure. This method has been shown to improve thermal regulation by gradually releasing stored heat during freezing conditions, thus enhancing the pavement's snow melting capacity [23, 24]. Another method involves embedding PCM within metallic pipes inside the concrete slabs. This technique allows for a higher concentration of PCM and can rapidly release heat during phase transitions, but it requires careful design to ensure even heat distribution and prevent thermal losses [25, 26].

OBJECTIVES AND SCOPE

The overall aim of this project is to develop practical pavement solutions that mitigate the UHI effect by reducing surface temperatures in pedestrian environments. The work focuses on integrating organic microencapsulated PCM into precast concrete sidewalks so that the pavement can store and release heat more efficiently, lower peak surface temperatures, and improve pedestrian thermal comfort, while remaining compatible with standard municipal materials and construction practices. This study established a proof of concept through thermal characterization and small-scale slab testing, and expanded the work to mechanical performance, numerical modeling, and full-scale field validation.

The specific objectives of this project:

- Advance innovative rigid pavement solutions using precast sidewalk elements with integrated organic microencapsulated PCM to help mitigate the UHI effect.

- Characterize the mechanical performance of PCM-integrated concrete mixes produced using both the addition and sand-replacement methods, including workability and compressive strength, to confirm their suitability for sidewalk applications.
- Improve understanding of the latent heat capability and thermal regulation behavior of PCM-enhanced concrete under repeated heating and cooling cycles by linking measured material properties with experimental results and numerical simulations.
- Support reductions in carbon emissions indirectly by lowering UHI intensity and improving the energy efficiency of buildings and urban infrastructure.
- Develop, refine, and validate a three-dimensional finite element thermal model capable of simulating multi hour heating and cooling cycles (2-hour, 4 hours, and 8 hour) for different PCM dosages and integration strategies.
- Construct and monitor a full-scale precast sidewalk pilot at the UTSA campus using multiple PCM percentages and surface treatments and evaluate its performance using a MCBI to capture cumulative cooling benefit over summer conditions.
- Integrate the mechanical, thermal, modeling, and field findings into practical guidance for agencies to design and deploy PCM-enhanced precast sidewalks within existing transportation infrastructure programs.

STUDY SCOPE

This study integrates material characterization, mechanical testing, numerical modeling, and a full-scale pilot sidewalk installation. Previously measured thermal properties and slab temperature history reported by (Radwan & Dessouky, 2024) are used as inputs to, and for validation of, the models and field interpretation. The scope of the current work is limited to the following components:

Experimental Work – Material-Based / Mechanical Analysis

- Produce concrete mixes with different PCM contents using both the addition method (percentage of total mix weight) and the sand-replacement method (PCM replacing a portion of the fine aggregate), at dosages up to 10 percent.
- Measure workability and slump of fresh PCM-integrated mixes to assess constructability for precast sidewalk production.
- Determine compressive strength at multiple ages (for example, 7, 14, and 28 days) to identify mixtures that provide adequate structural performance for sidewalk applications.

Experimental Work – Full-Scale Pilot Sidewalk

- Design, construct, and instrument a precast sidewalk test section on the UTSA campus consisting of six 4 ft × 4 ft segments produced using the sand-replacement method:
    - control concrete,
    - 5 percent PCM concrete,
    - sandblasted concrete without PCM,
    - sandblasted concrete with 2.5 percent PCM,
    - diamond-grinded concrete without PCM,
    - diamond-grinded concrete with 2.5 percent PCM.

- Monitor surface temperatures continuously over approximately three months (July through September 2025) to capture summer diurnal cycles, evaluate long-term cooling performance, and observe early-age aging effects under real weather exposure.
- Formulate and apply a MCBI based on measured surface temperatures to compare cumulative cooling benefits among the six sidewalk segments.

Numerical Modeling – Finite Element Analysis

- Develop a three-dimensional transient thermal finite element model in ABAQUS for control and PCM-enhanced concrete slabs, using the measured thermal properties from reported data in (Radwan & Dessouky, 2024) as input parameters.
- Calibrate the model against previously collected indoor and outdoor slab temperature history, including 8 hr. heating–cooling cycles, to ensure that PCM behavior (latent heat effects and reduced thermal diffusivity) is realistically represented.

Within this framework, the report focuses on the mechanical study, finite element modeling, and full-scale sidewalk testing completed during the project, while drawing on utilizing the previously measured thermal data for consistency and model validation.

> *It is worth noting that the study completed a full experimental program to evaluate the optimum PCM content of 5% sand-Replacement based on maximum thermal reduction and increased mechanical strength of concrete (Radwan & Dessouky, 2024)*

STUDY IMPACT

This study is expected to advance the use of organic PCM as a practical tool for mitigating the UHI effect in pedestrian-oriented infrastructure, with a particular focus on precast concrete sidewalks. By integrating material-level testing, numerical modeling, and full-scale field implementation, the work is anticipated to:

- Support the development of next-generation cool sidewalk systems that can be produced using familiar precast concrete practices while offering improved thermal regulation and enhanced pedestrian thermal comfort.
- Provide mechanical and modeling evidence that agencies can use to evaluate PCM-integrated mixes alongside conventional materials, helping decision-makers consider thermal performance as a design parameter in addition to strength and durability.
- Establish a finite element modeling framework that can be adapted by researchers, consultants, and agencies to explore different PCM dosages, surface treatments, slab geometries, and climate conditions before field deployment.
- Lay the groundwork for future guidelines, standards, and specifications that incorporate PCM-enhanced precast pavements and high-albedo surface treatments as part of broader climate-resilient and low-carbon transportation infrastructure programs.
- Encourage interdisciplinary collaboration among pavement engineers, urban planners, and sustainability professionals by framing sidewalks not only as structural elements, but also as active components of urban heat and energy management systems.

CHAPTER 2: LITERATURE REVIEW

INTRODUCTION

In the urban context, cities exhibit a temperature elevation of several degrees compared to rural and suburban areas, a phenomenon attributed to the interplay between the built environment and human activities. This thermal distinction, termed the UHI effect, emanates from divergent heat balances observed in building materials as opposed to natural ground surfaces [1], [2], [3]. The substantial thermal inertia and dark complexion of concrete materials are susceptible to the absorption and retention of solar radiation [4], [5], [6]. Solar absorption tends to be preferentially allocated to sensible heat rather than latent heat due to the inhibiting effect of impervious pavements on evaporative cooling [6], [7], [8]. The liberated sensible heat heats the urban atmosphere, playing a role in the formation of the UHI phenomenon. Given that pavements constitute 20–40% of the typical city's surface area [9], [10], the idea of using cool pavement to battle the UHI starts gained researched. Extensive research was undertaken to explore potential technologies and strategies aimed at cooling pavements, addressing key questions, ongoing research efforts, and areas where research gaps exist. The in-depth literature review is detailed in specific sections dedicated to each field studied in this study. This chapter offers a concise summary encapsulating the entirety of the literature review process.

URBAN HEAT ISLAND EFFECT

In essence, the term "heat island effect" delineates the distinctive higher temperatures observed in the atmosphere and surfaces within urbanized regions in contrast to their adjacent nonurbanized surroundings, typically encompassing underdeveloped or rural areas [11]. In cities hosting populations of 1 million or more, the average yearly air temperature can be notably higher, ranging from 1.8–5.4°F (1–3°C) compared to the neighboring areas [27]. Specifically, on clear and tranquil summer nights, this temperature differential can escalate significantly, reaching up to 22°F (12°C) [27]. The UHI phenomenon serves as an instance of inadvertent climate alteration resulting from the transformation of Earth's surface and atmospheric traits due to urbanization [28]. **Figure 1**, depicting the heat island, illustrates the typical scenario where urban temperatures tend to be lower at the periphery between urban and rural zones compared to the densely populated downtown areas. Additionally, the illustration highlights how green spaces such as parks, open lands, and water bodies contribute to creating cooler pockets within a city. Beyond the overarching city-wide impact on temperatures, the term "heat island" also encompasses a localized effect at specific sites. These localized effects refer to built-up areas that exhibit higher temperatures compared to their immediate surroundings, exemplified by scenarios like buildings, parking lots, or airports surrounded by open expanses with bare natural soil or vegetation. This phenomenon creates localized hot spots within the urban landscape. Typically, the local impact of heat islands tends to be significantly more intense compared to the broader global-scale effect. This heightened severity arises from the elevated local temperatures, resulting in more direct implications for pedestrians, buildings, and vehicles, as depicted in **Figure 2.** This study primarily concentrates on examining the site-specific localized effect of heat islands, acknowledging their immediate and pronounced influence within specific areas.

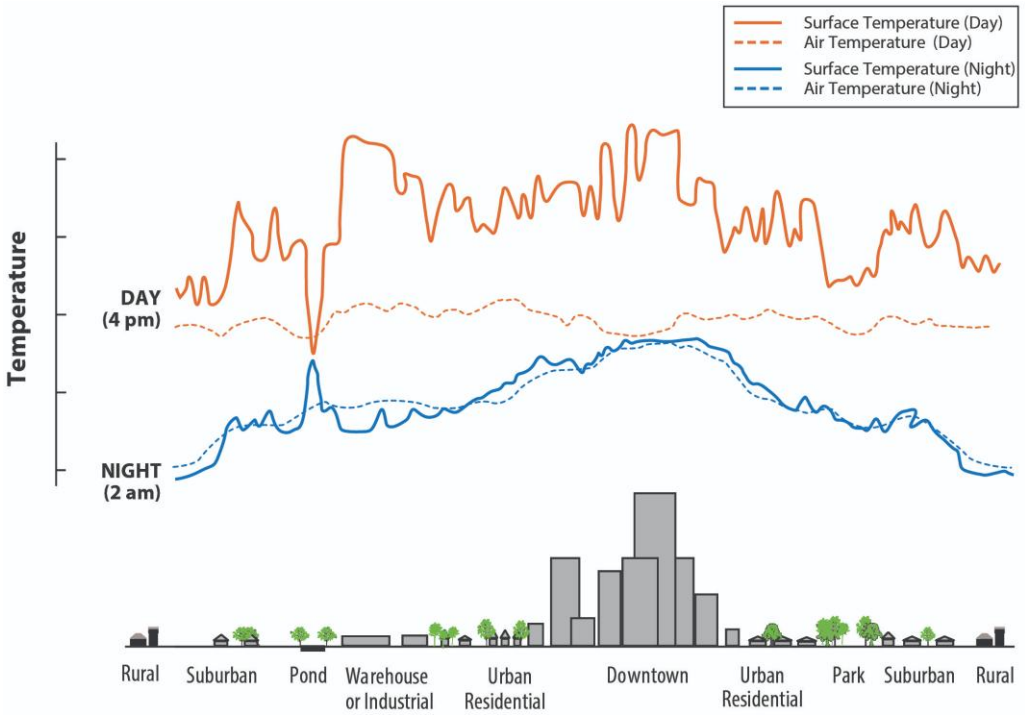

Figure 1: Heat Island sketch [27].

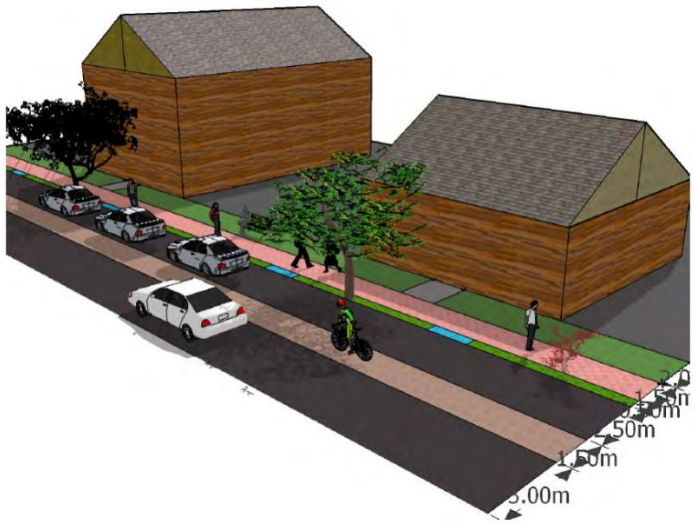

Figure 2: Localized pavement system with pedestrians, buildings, and vehicles [11].

The Impacts of Urban Heat Islands

In colder cities situated at greater latitudes or higher elevations, the warming impact of the heat island during winter is often perceived as advantageous. Additionally, in certain urban locales, the shade generated by tall buildings can create cooler zones for specific periods during the day, particularly in summer [11]. However, for the majority of cities, especially those with high population densities, the summer heat island's effects are regarded as problematic [28]. The

subsequent discussion focuses on regions characterized by hot summer climates. The heightened temperatures resulting from UHIs, notably during summer, can significantly influence a community's surroundings and overall living standards [11]. Although certain heat island effects may appear beneficial like extending the growing season for plants and cutting down on heating energy in colder regions the majority of these impacts are adverse [11]. Here is a list of the negative effects:

Compromised Human Health and Comfort

limited cooling at night, and increased air pollution levels can negatively impact human health. They contribute to general discomfort, respiratory issues, heat-related ailments like cramps, exhaustion, and non-fatal heat stroke, as well as heat-related fatalities [11]. Heat islands worsen the effects of heat waves, characterized by extremely hot and often humid weather. Vulnerable groups like children, older adults, and those with existing health conditions face heightened risks during these events. Abrupt temperature spikes, termed excessive heat events, pose severe dangers, leading to premature deaths and potentially higher mortality rates [11]. Apart from health impacts, discomfort caused by pavement heat might discourage walking or biking, reducing physical activity and short-distance travel on foot or bike, which can affect public health. This shift from walking or biking to driving could hinder efforts to build sustainable, livable, and walkable communities [11].

Increased Energy Use

Research conducted by LBNL [14], [27] highlights that for each 1°F (0.6°C) rise in air temperatures between 68 and 77°F (20 to 25°C), there is a 1.5-2.0% surge in electricity demand for building cooling. This indicates that roughly 5-10% of the overall community-wide electricity consumption is allocated to offsetting the heat island effect. Moreover, beyond the amplified energy use for cooling buildings, higher temperatures might also increase the need for cooling vehicles when they are parked or traveling on heated pavements for extended durations. The UHI has the potential to elevate both peak and total electricity demand, typically happening during hot summer weekdays. This surge aligns with the simultaneous operation of cooling systems, lights, and other appliances in offices and homes during afternoon hours [11]. As previously mentioned, the extent of this effect relies on the local climate where pavements are used and the nature of the built environment surrounding these pavements [11]. However, comprehensive studies evaluating the overall impact of entire UHI effects are limited, and there is a scarcity of specific studies examining the localized heat island effects caused by pavement heat.

Increased Release of Air Pollutants and Greenhouse Gases

Previously noted, UHIs heighten energy demand in summer, with electricity suppliers in the U.S., China, and India relying heavily on fossil fuel plants to meet this need. Consequently, this reliance leads to increased emissions of harmful pollutants sulfur dioxide (SO2), nitrogen oxides (NOx), particulate matter (PM), carbon monoxide (CO), and mercury (Hg) [29]. These pollutants pose health risks and contribute to complex air quality issues, including ground-level ozone, fine particulate matter, and acid rain. Moreover, the heightened use of fossil fuel plants escalates greenhouse gas emissions, notably carbon dioxide (CO2), exacerbating global climate change [11]. Additionally, warmer temperatures directly hasten ground-level ozone formation, resulting from the interaction between nitrogen oxides (NOx) and volatile organic compounds (VOCs) in sunlight

and hot conditions [30]. In hotter climates, given similar conditions like precursor emissions and wind speed, there is an increased formation of ground-level ozone [29].

The Lifespan of a Pavement

Pavement temperatures play a crucial role in determining pavement durability. In hot climates, asphalt pavements face increased risks of rutting (permanent deformation), aging, and cracking during summer if not designed to withstand high temperatures [17], [31]. Similarly, for concrete pavements, elevated temperatures and temperature variations can raise the likelihood of cracking due to thermal stress [32], [33]. However, the impact of temperature on pavement durability varies depending on the pavement type. Additionally, the precise effects on certain pavements, like permeable pavements, remain unclear. Implementing cool pavements and associated cooling technologies has the potential to lower pavement temperatures and temperature variations, potentially enhancing pavement durability by mitigating thermal-related damage such as rutting or cracking [11]. Overall, this approach could reduce pavement maintenance expenses and offer additional benefits such as decreased material usage and reduced traffic delays for users. The importance of heat islands and pavement heat hinges on various factors like local climate, urban area size, building density affecting wind flow, pavement coverage, and nearby air conditioning use [11]. Despite their potential impact, there is a scarcity of comprehensive studies on the overall effects of heat islands, and few specifically delve into the impact of pavement heat. Furthermore, these effects vary in significance across locations, and there is a lack of systematic, location-specific data detailing these consequences [11].

Factors Contributing to Heat Islands

To uncover the reasons behind the heat island phenomenon, comprehending the concept of the "energy balance" at the Earth's surface and the primary heat transfer mechanisms is valuable [11]. This knowledge aids in identifying and gaining deeper insights into the fundamental drivers of heat islands as shown in **Figure 3.** As previously discussed, the heat island is not attributed to a singular cause. Instead, multiple factors converge, collectively elevating temperatures in cities and suburbs, detailed in **Table 1** [28]**.**

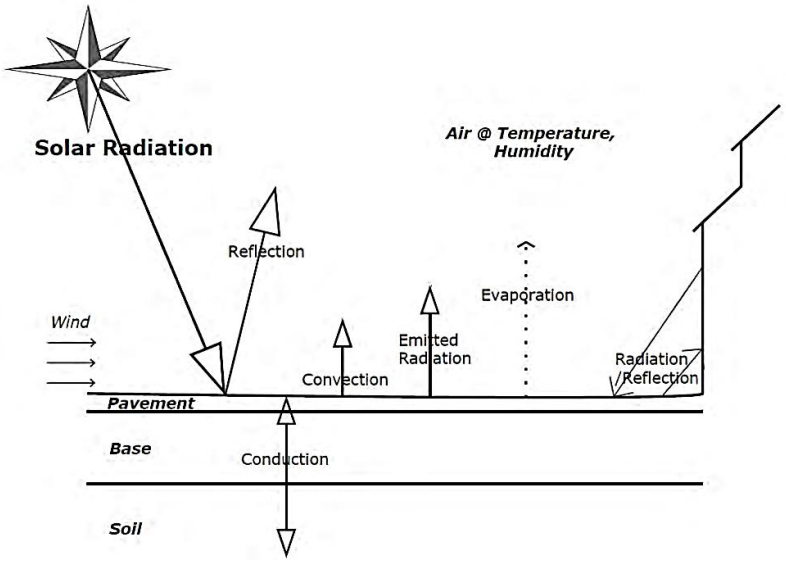

Figure 3: Energy balance on pavement surface [11].

Table 1:Characteristics to heat island formation and their effects on the energy balance [28].

Characteristic contributing to heat island	Effect on the energy balance
Lack of vegetation	Reduce evaporation
Widespread use of impermeable surfaces	Reduce evaporation
Low solar reflectance of urban materials	Increase net radiation
Urban geometries that trap heat	Increase net radiation
Urban geometries that slow wind speeds	Reduce convection
Increase energy use	Increase anthropogenic heat

COOL PAVEMENTS

Cool pavements can be achieved through various methods, such as modifying existing pavement materials, employing innovative designs, or introducing new materials into traditional pavements [34], [35]. Pavements maintain cooler temperatures compared to conventional ones by enhancing solar reflectance, promoting evaporation, and decreasing the sensible heat released into the urban atmosphere. These cooling techniques are often referred to as reflective pavements, evaporative pavements, and heat-harnessing pavements. Reflective pavements, for instance, have higher albedo, aiding in reducing surface temperatures and releasing less sensible heat [36], [37], [38] Evaporative pavements retain water in surface or lower layers for evaporative cooling, maintaining lower temperatures [39], [40]. On the other hand, heat-harnessing pavements mitigate surface temperatures by using absorbed heat as renewable energy for other purposes [41], [42], [43]. The discussion on cool pavements extends beyond cooling techniques to examine their impact on urban climates. Some studies delve into the benefits, drawbacks, costs, and policies associated with cool pavements [36], [44], [45]. This review offers an overview of cool pavements, touching on various aspects but not aiming to cover every facet comprehensively. Instead, it aims to showcase techniques and advancements in cool pavement research. Topics include definitions of cool pavements, their techniques and functioning, their influence on pavement temperature and the urban environment, as well as their benefits, drawbacks, costs, and policy implications. The focus lies particularly on reflective and evaporative pavements and their potential in addressing the (UHI) effect. Additionally, research gaps between cool pavements and their effects on the urban environment are discussed, and potential avenues for future research are proposed. **Table 2** summarizes most of the cool pavement techniques.

Table 2: Summary of cool pavement types [46].

Modifications	Cool techniques	Category	Construction
Absorption	Reduce heat absorptivity by reflecting solar radiation to the sky. Make the surface reflective at hot weather and absorptive at cold weather	• Reflective Asphalt pavement • Reflective concrete pavement • Thermochromic pavement with doped reflective pigments	Surface treatment or reconstruction

Evaporation	Increase latent heat release	• Porous pavement, permeable pavement, and pervious pavement. • Water-retentive pavement	Reconstruction
Storage	Extract heat from pavement and reduce surface temperature. Reduce surface temperature by increasing conductivity heat	• Heat-harvesting pavement. • PCM-impregnated pavement and high-Conductive pavement	Reconstruction

Reflective Asphalt Pavement

The method entails the application of a thin layer of hot bitumen onto existing pavements, integrating finely graded aggregates. This process creates a reflective surface influenced by both the color of the aggregates and the aging of the pavement [47]. Research findings suggest that while the reflectance of chip seal pavement diminishes over time, it remains higher than that of standard asphalt concrete for approximately five years [48]. While light-colored slurry seal treatments also enhance pavement reflectance, their usage is restricted due to the requirement of reformulating emulsifiers for achieving the necessary whiteness, thereby increasing costs [45]. Alternative techniques, such as applying light-colored paint or incorporating light-colored materials into micro-surfacing, significantly bolster the reflectivity of asphalt pavements [49]. However, these highly reflective surfaces, while proficient in bouncing back visible light, might result in glare and pose aesthetic concerns. Recent advancements involve the application of nonwhite pigments that reflect high near-infrared light to coat pavements. Detailed information regarding the thermal properties of pavements utilizing these high near-infrared reflectance pigments is scarce, although insights from cool roof tiles provide relevant knowledge [50], [51], [52], [53]. Over time, exposure and weathering may lead to the degradation of the coating's reflective properties [54].

Reflective Concrete Pavement

Concrete pavements can achieve high reflectivity by incorporating whitish cementitious materials and light-colored aggregates. Among these components, the solar reflectance of the cement plays a primary role in determining the concrete's albedo, with other constituent materials contributing secondary effects [55]. As Portland cement hydrates, the albedo increases due to the production of calcium hydroxide, stabilizing after the completion of hydration [56]. Incorporating fly ash enhances concrete durability but might slightly decrease albedo, likely because fly ash is darker than Portland cement. Conversely, pozzolanic additive slag increases albedo as it has higher reflectance than fly ash [55], [57]. Factors such as wetting, soiling, and abrasion affect the solar reflectance of concrete samples after exposure [56]. At the aged stage, the albedo primarily depends on the reflectance of fine aggregates and paste [55], [56]. White-topping and roller-compacted pavements also exhibit high reflectivity. White-topping involves resurfacing distressed pavements with a concrete overlay, typically referring to four or more inches of concrete laid over existing asphalt pavements. Ultra-thin white-topping, on the other hand, entails a two to four-inch overlay specifically designed for low-traffic urban streets [58].

Evaporative Pavements

Pavement systems such as roads, parking lots, and walkways can be engineered to retain water, aiding in evaporative cooling. These pavements maintain lower temperatures as they absorb less solar energy for thermal conduction compared to dry pavements. Water-retaining pavements are typically categorized as porous paver, permeable paver, and pervious paver [59].

Porous Pavers

The porous pavers have internal cavities that allow water to permeate through them. These pavers typically consist of a cellular grid structure where these cavities are filled with substances like dirt, sand, gravel, or grass to retain moisture. The proportion of this filling material usually ranges from 20 to 50% of the total pavement area [59]. If materials like dirt, soil, or gravel are used, the cooling effect may be minimal, making the system thermally similar to a concrete pavement. However, when grass is utilized, it encourages transpiration, and its root system transports moisture from deeper soil layers to the surface, facilitating evaporation and cooling of the pavement [60].

Permeable Pavers

Permeable pavers, also known as permeable modular pavers, consist of a layer of concrete or fired-clay bricks [59]. Unlike pervious and porous pavers, these structures enable rainwater to pass around them rather than through. The pavers feature spacing lugs or small apertures, creating channels for water evaporation stored in the surface and lower layers. Typically, these lugs have an area ratio of 8–20%. Observations on the temperature variations of permeable pavers yield diverse results. Asaeda and Ca [60] found that these pavers exhibit temperatures similar to concrete pavement. However, they tend to be warmer during the day and cooler at night compared to asphalt pavement. In contrast, Andersen et al. [61] observed varying evaporation rates, ranging from 0.09 to 0.22 kg/m²/day, approximately equivalent to 9–22 W/m² during midday if nighttime evaporation is negligible. This implies that permeable pavers provide limited evaporative cooling. Theoretically, when dry, permeable pavers possess lower thermal inertia and reduced surface reflectance due to their rough texture compared to dense pavements. A dry permeable pavement should be hotter than a dense pavement during the daytime. Hence, the cooling effect of a permeable pavement depends on whether the evaporative flux surpasses the additional heat gain resulting from its low thermal inertia.

Pervious Pavers

Pervious pavers, a distinct type of concrete, boast high porosity that enables water to pass directly through rather than around them. Constructed with concrete paste or asphalt binder coating large, single-graded aggregates [62], these pavers feature cavities that facilitate water drainage. Pervious concrete exhibits water permeability ranging from 10^8 to 10^10 m² (about 9.7 × 0.0097 cm/s), with most of the percolating water not retained within the pavers as they swiftly drain [63]. The cooling efficiency of pervious pavements remains a subject of debate in literature. Some observations note that on sunny summer days, pervious pavements can be as hot as dark asphalt pavements due to their higher solar absorption and lower thermal inertia compared to conventional pavements [60]. Conversely, other studies suggest that pervious pavements display lower temperatures at nighttime and can cool faster than regular concrete, potentially qualifying as "cool" pavements [64].

Information on the thermal properties of pervious concrete is limited. Firstly, there are few reports on the reflectance of pervious concrete [65]. The roughness of its surface results in a lower albedo compared to regular concrete, leading to increased solar absorption [65]. Secondly, specific measurements regarding the thermal properties of pervious concrete are scarce. Although known for possessing lower thermal inertia than traditional concrete, there are no definitive measurements reported to date. Thirdly, the heat convection characteristics of pervious concrete remain less understood. The surface's roughness may contribute to a higher heat convective coefficient, potentially enabling it to stay cooler than normal concrete in windy conditions [55]. Lastly, pervious concrete's porosity, ranging from 15%–30% or more [40], might induce buoyancy-driven convective cooling within the cavities when there is a significant temperature gradient. Studies on the evaporation of pervious concrete are also limited [66]. Experiments by Nemirosky et al. [67] quantified the evaporation of pervious concrete samples in the lab under diurnal cycles of artificial solar irradiation. The experiment involved various water ponding depths to simulate undrained pervious pavement bases. Results indicated substantial evaporation when water was ponded close to the surface, contributing to decreased pavement temperatures. However, deeper water levels compromised evaporation and provided limited cooling effects. Additionally, observations suggest that unless properly re-wetted within an appropriate timeframe, the evaporation of pervious concrete contributes minimally to surface temperature reduction.

Water-Retaining Pavements

Water infiltrates through pervious concrete at a rapid pace, hindering its ability to retain an optimal amount of water for evaporative cooling. Consequently, water-retentive pavements, whether asphalt- or cement-based, were developed to specifically retain water primarily at the top layer. Various terminologies like water-holding, water-retentive, watered, or water-retaining pavements are used to describe this type of pavement in documented literature. While water-retentive pavements exhibit porosity comparable to permeable pavements, their water permeability ranges between 10^-11 to 10^-13 m^2, which is one or two magnitudes lower than that of permeable pavements (10^-8 to 10^-11 m^2) [68]. To retain significant amounts of water, these pavements embed water-retentive fillers like blast-furnace slag, pervious mortar, bottom ash, peat moss, hydrophilic fiber, and other water-absorbing materials [68]. Depending on the filler, a water-retentive pavement can retain approximately 0.15–0.27 g/cm^3 (equivalent to 15 kg/m^2) of rainwater when the surface is adequately wet [69]. Numerous research endeavors aim to enhance the evaporation capacity of water-retentive pavements. One approach involves replenishing these pavements with wastewater. In cities like Tokyo and Osaka, wastewater has been sprinkled on water-retentive pavements to prolong evaporative cooling [46]. Large-scale experiments conducted in Shio Site, Tokyo, installed water-supplied pipes along the pavement to automatically spray reclaimed water. These efforts have demonstrated that sprinkling reclaimed water helps maintain cooler temperatures in comparison to planted zones [69]. Other strategies to augment the cooling potential of water-retentive pavements involve utilizing highly absorptive fillers and novel pore structure designs [46].

PHASE CHANGE MATERIALS (PCMS)

The recent introduction of PCMs has aimed to enhance the thermal properties of building materials [70]. These substances are adept at storing and releasing significant thermal energy during phase transitions. Classified into organic, inorganic, and eutectic mixtures, PCMs have been integrated into materials like concrete and gypsum, notably amplifying their thermal mass. This

augmentation plays a crucial role in moderating indoor temperatures, facilitating energy conservation in buildings. Beyond their impact on energy efficiency, PCMs also exhibit potential to improve mechanical and durability aspects of construction materials [71]. For example, studies explore their ability to regulate temperature variations and heat evolution in concrete during hydration, enhance crack resistance, and minimize thermal shrinkage. Researchers have also investigated their role in reducing thermal stress and damage in concrete pavements subjected to freezing-thawing cycles or temperature gradients. Yet, the incorporation of PCMs in building materials, particularly concrete, is not without challenges [24]. Concerns about potential PCM leakage in liquid states have arisen, posing risks such as interference with cement hydration and adverse effects on concrete's mechanical properties. Consequently, various methods have been proposed to safely incorporate PCMs into building materials and prevent leakage when in a molten state [24]. These methods, broadly categorized as microencapsulation, SSPCMs, porous aggregate inclusions, and macro-encapsulation, require careful consideration of their specific applications and their influence on the host material's characteristics. **Figure 4** outlines the main features associated with each incorporation method.

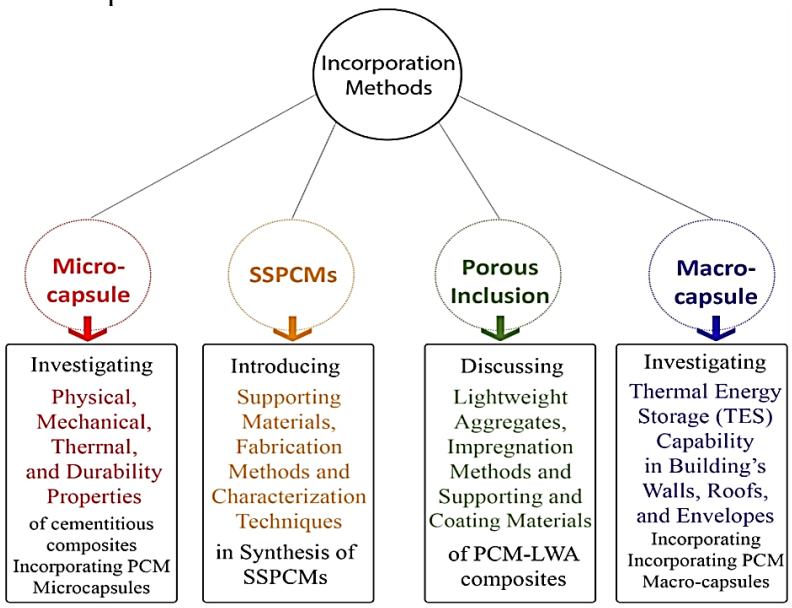

Figure 4: Categorization of different methods of PCM incorporation into construction materials and their associated technical considerations [72].

Microencapsulation Techniques

Microencapsulation stands as a highly effective approach for integrating PCMs into building materials. Beyond shielding against PCM leakage during the melting phase, this method significantly enhances thermal conductivity, optimizing PCM performance across melting and freezing cycles. The diverse techniques for PCM microencapsulation fall into three primary categories: physical, physicochemical, and chemical methods [73]. Recent advancements have yielded various commercially available microcapsules tailored for the building industry. The predominant application of PCM microcapsules lies within cementitious composites, prompting numerous studies investigating PCM-infused cementitious materials [72]. Typically, PCM microcapsules are directly integrated into the concrete mixing process, often serving as a partial substitute for sand. This strategy has garnered attention due to its potential to enhance the thermal properties of concrete and expand its applications in building materials [72].

Shape Stabilization Of PCM

The risk of PCM leakage during its molten state and its potential environmental impact have prompted researchers to propose a novel solution known as shape-stabilized PCMs (SSPCMs) [72]. This innovative approach involves stabilizing PCMs in their molten form through a supporting material (SM). Similar to microencapsulation, shape stabilization not only prevents PCM leakage but also enhances the thermal conductivity of the composite, improving its behavior across melting and freezing cycles [72]. The choice of SM and the technique employed for SSPCM fabrication play pivotal roles in influencing thermal characteristics. Typically, three primary methods are employed for SSPCM fabrication: direct absorption, vacuum impregnation, and sol-gel methods. It is important to note that the addition of SM can induce alterations in the thermo-physical properties of PCMs. Hence, comprehensive characterization of fabricated SSPCM composites is essential [72]. Experimental evaluation of the impact of SSPCMs on both thermal and mechanical properties of the host construction material is imperative. **Figure 5** provides a concise categorization of influential factors in the fabrication of SSPCMs. Critical examination of fundamental experiments for characterizing SSPCMs is also imperative. Within this context, a discussion ensues regarding the most significant SMs and applied fabrication methods for SSPCMs. Furthermore, emphasis is placed on fundamental experiments aimed at characterizing SSPCMs and evaluating their effects on both thermal and mechanical properties of the host construction material [72].

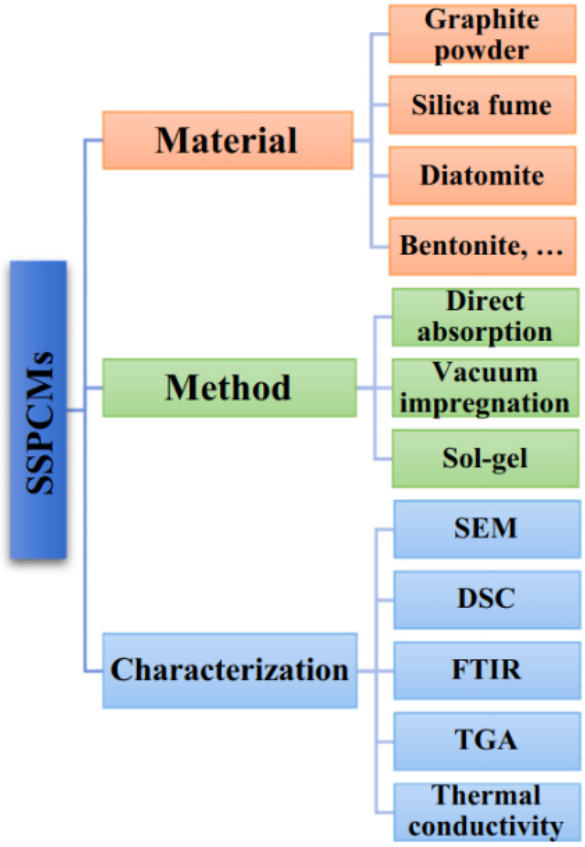

Figure 5: Influential factors in the fabrication of SSPCMs [72].

Porous Inclusion

This method of infusing PCMs into concrete by absorbing them into porous LWAs is both intriguing and practical. It shares similarities with shape-stabilizing techniques but stands out due to certain key differences. Unlike the approach with SSPCMs, where PCMs substitute fine aggregates in the concrete mix, PCM-LWA involves a distinct method [74]. Specifically, the supporting material (SM) used for PCM-LWA differs from that in SSPCMs. While SSPCMs usually employ powder materials like graphite or silica fume as the SM, PCM-LWA relies on porous aggregates characterized by larger size and robust mechanical strength, promising enhanced concrete performance. Several critical factors influence the effectiveness of PCM-LWA concrete and demand meticulous consideration while determining mixture proportions. These factors encompass the type of LWA and its absorption capacity, the impregnation method, the coating and supporting materials, as well as comprehensive characterization and performance testing [75]. Researchers have explored diverse porous aggregates such as PCM hosts, various impregnation techniques, and an array of coating and supporting materials. This method offers a promising pathway for integrating PCMs into concrete through PCM-LWA, offering distinct advantages over conventional shape-stabilizing approaches. Its emphasis on using porous aggregates capable of effectively housing PCMs holds the potential to significantly enhance concrete's thermal properties. Rigorous attention to these influencing factors remains pivotal in optimizing PCM-LWA concrete's performance for practical applications.

Macro-Encapsulation

Integrating PCMs into construction materials is vital for enabling Thermal Energy Storage (TES) systems via PCM latent heat capacity. Consequently, PCMs have been integrated into various construction materials, including concrete and gypsum, as well as in different architectural elements like walls and roofs [74]. To counter potential negative impacts of PCMs on mechanical properties, researchers have developed diverse strategies that prevent direct contact between PCMs and the integrated construction materials. Among these strategies, macro-encapsulation emerges as a particularly effective approach, notably suited for incorporating PCMs into elements such as prefabricated walls and roofs. In this method, PCM remains distinct from the primary construction material (e.g., concrete or gypsum), preserving the mechanical strength of the base material. Importantly, this separation does not compromise the substantial thermal advantages that PCMs offer to these building components. Interestingly, different references might classify PCM incorporation methods differently; for instance, some view PCM impregnation within LWA as a form of macro-encapsulation [76]. Additionally, alternative PCM forms like PCM microcapsules or Shape-Stabilized PCMs (SSPCMs) can also be utilized to create macro-encapsulated PCM elements [77]. Recent studies have explored scaled-down experimental methods and empirical approaches to comprehensively evaluate the thermal response of PCM-integrated building components [78]. Furthermore, extensive numerical analyses have investigated how PCM inclusion impacts building components and the overall energy consumption of buildings [79]. **Figure 6** illustrates the schematic of hollow core slab filled with PCM [80].

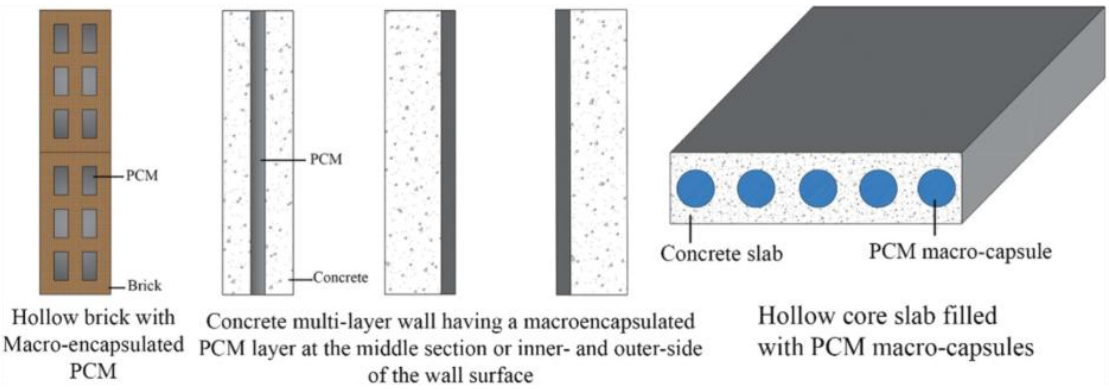

Figure 6: Schematic cross-section of PCM macro-encapsulated wall and floor configurations [80].

PCM in Pavements

The integration of PCMs into pavement materials has become an area of significant interest due to their potential to regulate extreme temperatures and enhance pavement durability. PCMs have the unique ability to absorb and release thermal energy during phase transitions, which can mitigate the (UHI) effect and reduce thermal stresses in pavements.

Incorporation Of PCM In Asphalt Pavements

Ma et al. [81] explored the impact of Shape-Stabilized PCMs (SSPCMs) on asphalt pavements. Their findings suggest that integrating (SSPCMs) can mitigate temperature-related challenges in asphalt pavements. While they reported enhanced resistance to low-temperature cracking, both Marshall stability and dynamic stability declined as the PCM dosage increased. In a subsequent study by Ma et al. [82], it was demonstrated that (SSPCMs) effectively lowers the maximum pavement temperature during heating and raises the minimum pavement temperature during cooling. Although the temperature peaks of specimens with and without SSPCMS occurred at roughly the same time, it was concluded that (SSPCMs) does not affect the timing of peak temperature in asphalt. However, more detailed research by Ma et al. [83] revealed that PCM in pavement does influence the timing of extreme temperature occurrences. Specifically, the use of PCM delayed the occurrence of maximum and minimum pavement temperatures by 30 minutes and 20 minutes, respectively. The study also compared the cooling rates of asphalt with and without PCM in negative temperature environments. A faster cooling rate leads to a higher shrinkage strain rate, increasing the likelihood of transverse cracks. It was observed that the cooling rate of asphalt pavement with PCM was slower than that of pavement without PCM. Chen et al. [84] examined the effect of PCMs on the rutting performance of asphalt pavements, concluding that PCM addition can significantly enhance the rutting resistance of asphalt, there is a sharp decline in dynamic stability at 48–52°C for base asphalt and at 55–60°C for PCM-modified asphalt. This decline occurs when the pavement temperature surpasses the softening point of the asphalt. Thus, the study recommended maintaining the peak phase change temperature 3–5°C below the asphalt's softening point. In a later study, Chen et al. [85] evaluated the effect of PCM on the thermal and mechanical properties of asphalt mixtures. The research utilized an asphalt binder with a softening point of 48.5°C and two different PCMs with melting temperatures of 50°C (PCM 50) and 45°C (PCM 45). The volumetric heat capacity of the asphalt mixture containing PCM 50 was relatively higher. Since mixtures with higher heat capacity can store more heat, PCM 50 was considered more effective in controlling asphalt pavement temperature. Although the

samples with PCM 50 and PCM 45 satisfied the standard specifications for rutting parameters, there was a reduction in dynamic stability by 9.7% for PCM 50 and 61% for PCM 45 compared to the control sample.

Incorporation Of PCM In Concrete Pavements

Dehdezi et al. [116] focused on the thermal, mechanical, and microstructural properties of concrete pavements that incorporated micro-encapsulated paraffin wax as PCM, with particle sizes ranging from 20 to 80 micrometers. Although the microstructural analysis showed that the PCM remained intact during mixing and curing, it was observed that the particles burst under loading conditions. This bursting significantly increased the porosity of the concrete, which adversely affected its mechanical strength. Despite the concrete's satisfactory thermal performance due to PCM integration, the compromised mechanical strength limits its suitability for pavement applications. Ma et al. [86] introduced composite shape-stabilized PCM (CS-PCM) for managing low-temperature conditions in concrete pavements. They selected tetradecane (C14H30) as the PCM, given its phase change temperature aligns with the temperatures that cause low-temperature pavement distress. The PCM stabilized with ethyl cellulose as the membrane material and either activated carbon or silica as carrier materials, with silica being the preferred choice due to its higher theoretical enthalpy. A custom dispersion agent was used to improve the distribution of the carrier material, enhancing the heat storage capacity, and preventing the clustering of SSPCMs particles. The optimal mixture ratio was determined to be 1:1:0.1:0.1 for tetradecane, silica, ethyl cellulose, and dispersant, respectively. In a different approach, Farnam et al. [87] examined the use of LWA and embedded tubes to incorporate PCM into concrete pavements. Plastic pipes with a 10 mm diameter were used as embedded tubes, and two types of PCMs were employed: paraffin oil (petroleum-based) and methyl laurate (vegetable-based). When paraffin oil was incorporated into LWA, it released 11,000 kJ/m³ of heat at around 3.0°C during freezing. However, methyl laurate did not release any heat due to a chemical reaction with the cementitious material. In the case of mortar with embedded tubes, paraffin oil and methyl laurate released 7,500 kJ/m³ of heat at roughly 3.0°C and 12,000 kJ/m³ of heat at around 1.2°C, respectively. Importantly, the integration of PCM into embedded pipes did not trigger any chemical reactions. Later, Farnam et al. [21] replaced the plastic pipes with carbon steel pipes, which had a 22.4 mm inner diameter, 0.5% carbon content, and a thermal conductivity of 45 W/mK to accommodate the maximum aggregate size of 19 mm, a spacing of 25 mm was maintained between the pipes. This configuration enabled the PCM-enhanced concrete slab to melt 136.9 mm of snow within the first 24 hours. Meanwhile, Yeon and Kim [88] explored a method to improve freeze-thaw resistance in concrete pavements using PCM microencapsulated with melamine-formaldehyde resin, produced via an emulsification process. Due to the significant cost increase associated with producing microencapsulated PCM in powder form, they opted to use it in slurry form instead. The liquid phase of the slurry functioned as free water, necessitating adjustments to the water content in the concrete mix. Their results showed that the addition of PCM significantly enhanced the pavement's resistance to freeze-thaw damage. However, it was also noted that PCM's effectiveness decreased when the ambient temperature remained lower than the phase change temperature for extended periods, as the PCM would fully solidify and reach thermal equilibrium with its surroundings. In such situations, it is recommended to use a PCM with a lower phase change temperature.

SUMMARY

Chapter 2 focuses on the literature review, providing an in-depth analysis of the UHI effect and strategies for mitigating it, specifically through the use of PCM in pavements. The review covers how urban areas experience significantly higher temperatures than rural regions due to the properties of concrete and other urban materials, which absorb and retain heat. This chapter explains the UHI effect's contribution to increased energy consumption, compromised human health, and elevated greenhouse gas emissions. Various cooling strategies, such as reflective pavements, evaporative pavements, and the use of porous or permeable materials, are explored as potential solutions. Additionally, it discusses the integration of PCMs into pavement materials, focusing on their ability to absorb and release heat during phase transitions, thereby reducing surface temperatures. Several studies are referenced that explore different encapsulation techniques, such as microencapsulation and shape stabilization, highlighting their effectiveness in enhancing the thermal properties of concrete. The chapter sets the groundwork for understanding how incorporating PCM into concrete pavements can mitigate UHI effects and improve the sustainability of urban infrastructure.

CHAPTER 3: METHODOLOGY

This chapter describes the experimental and numerical methods used to evaluate PCM integration in precast concrete sidewalks for UHI mitigation. The methodology is organized into three main components. First, a mechanical study was conducted to verify that PCM-integrated concrete mixes produced by both the addition and sand-replacement methods satisfy strength and workability requirements for sidewalk applications. Second, three-dimensional transient finite element (FE) thermal models were developed and calibrated using previously measured thermal properties and slab temperature histories to simulate multi-hour heating–cooling cycles for different PCM dosages and integration strategies. Third, a full-scale pilot sidewalk was designed, constructed, and instrumented on the UTSA campus using the sand-replacement method with multiple surface treatments and PCM percentages, providing field data for model validation and practical implementation guidance.

Mechanical Phase: Compressive Strength and Workability

Mechanical testing was conducted to ensure that integrating organic microencapsulated PCM into the concrete mix does not compromise the structural integrity required for TxDOT-type sidewalk concrete. Cylindrical specimens with a nominal size of 4 in. diameter × 8 in **(Figure 7).** height were cast using the control mixture and PCM-modified mixtures at different replacement levels (e.g., 5% and 10% by weight of the control mix), for both the sand-replacement and addition methods. For each PCM level and mixing method, three replicate cylinders were prepared. Fresh concrete was mixed in the UTSA materials laboratory using the same binders and aggregates as in the thermal phase, with PCM dosages adjusted according to the target mix design. The water-to-cement ratio and admixture contents were chosen to be compatible with TxDOT sidewalk concrete practice and then held constant so that the influence of PCM could be isolated. Workability was monitored during casting by observing slump, ease of placement, consolidation, and finishing, noting any changes in stickiness or segregation relative to the control mixture. After casting, all cylinders were demolded after 24 hours and cured by full immersion in a lime-saturated water tank in accordance with ASTM C39/C39M-23, which specifies curing and testing procedures for cylindrical concrete specimens subjected to compressive loading. Compressive strength tests were

carried out at selected ages (e.g., 7 and 28 days) using a calibrated compression testing machine, and strength values were calculated as the maximum load divided by the cross-sectional area. For both the addition and sand-replacement PCM methods, the measured compressive strengths and observed slump/workability were directly compared with Texas Department of Transportation design expectations for sidewalk concrete (minimum compressive strength and workable slump range). Mixes that did not meet these TxDOT-type performance targets were considered unsuitable for field implementation, even if they showed favorable thermal behavior. This comparison highlighted that higher PCM contents in the addition method result in more pronounced strength reductions and lower workability than comparable sand-replacement mixes, guiding the choice of mixes for the field sidewalk.

Figure 7:Compressive Strength Testing of 4x8 inch concrete cylinders

Finite Element Thermal Modeling

To generalize the experimental findings and explore additional operating scenarios, three-dimensional transient thermal finite element models of the PCM concrete slabs were developed in ABAQUS **(Figure 8).** The slab geometry and boundary conditions replicated the indoor reflective thermal box: a rectangular concrete slab elevated above the chamber floor and heated by two 250-W infrared bulbs mounted above the surface. Concrete was modeled as a homogeneous, isotropic material with temperature-dependent thermal properties calibrated from the measured thermal conductivity, diffusivity, and heat capacity of the control and PCM-modified concretes. For each integration method (addition and sand-replacement) and dosage (0%, 5%, and 10% PCM), separate material definitions were assigned so that the FE model reflected the measured increase in heat capacity and reduction in thermal conductivity produced by PCM integration. The model used 20-node quadratic hexahedral elements (DC3D20) through the slab thickness. A mesh-sensitivity study was performed; the selected mesh (Mesh 10) contained 6072 nodes and 1125 elements **(Figure 9, Table 3),** which provided converged maximum surface temperatures with acceptable computational cost. Heat transfer between the slab and its surroundings was modeled using

radiation and natural convection. Radiative heat input from the bulbs was calculated using the inverse-square law, based on the 500-W total bulb power, distance from the bulb to the slab surface (0.4572 m), and the exposed surface area (0.06 m²), and applied as a uniform surface heat flux on the top surface of the slab. A convective boundary condition of 15 W/m²·K was applied to the slab surfaces to represent natural convection inside the insulated chamber. Because the slab was elevated, direct conduction to the supporting base was neglected, while internal conduction within the slab was captured by the transient heat-conduction formulation in ABAQUS.

Two sets of transient simulations were performed for each material configuration:

- Four-hour cycle: 2 hr. heating followed by 2 hr. cooling.
- Eight-hour cycle: 4 hr. heating followed by 4 hr. cooling.

For each simulation, nodal temperatures at locations corresponding to the thermocouples on the top and bottom slab surfaces were extracted at one-minute intervals. These were compared to the indoor experimental temperature histories for the corresponding PCM content and mixing method. Model performance was evaluated using root-mean-square error (RMSE) and peak temperature differences between measured and simulated responses, and the calibrated model was then used to explore additional PCM dosages and climate scenarios beyond those tested experimentally.

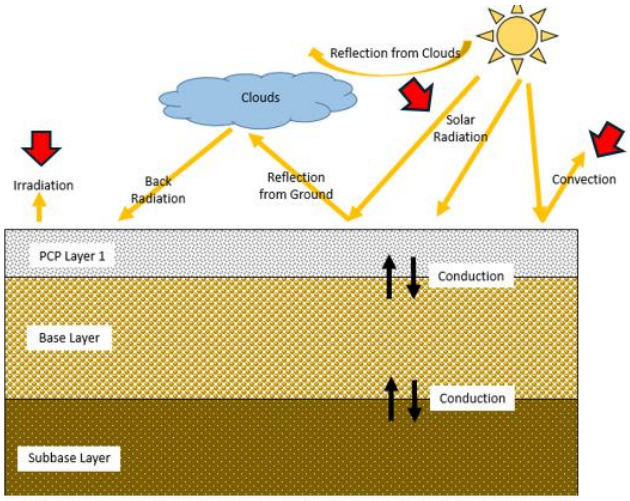

Inverse Square Law:

$E = P / (4\pi r^2)$

Rectangular Area Calculation:

$A = L \times W$

Incident Power Calculation:

$P_{(incident)} = E \times A$

Where:

- Total bulb power: 500 watts
- R is Distance from source to surface: 0.4572 meters
- Surface area: 0.06 m²

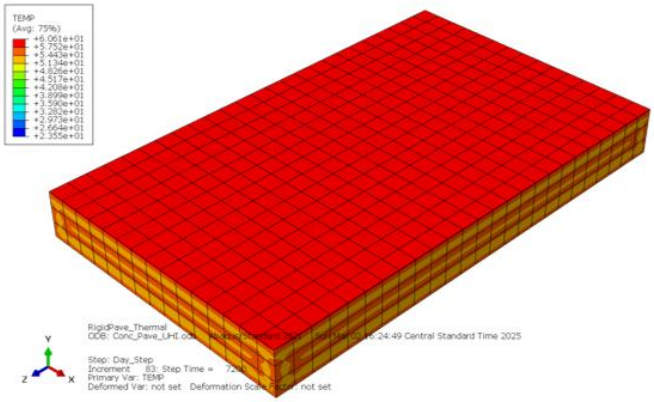

Figure 8: Finite Element Modelling Configurations

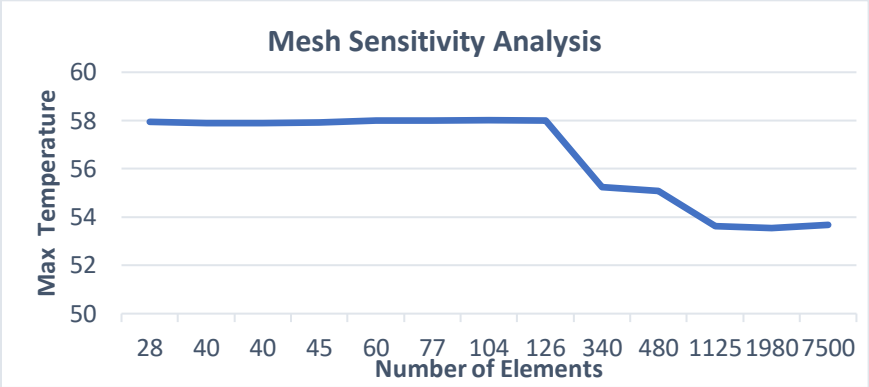

Figure 9: Mesh Sensitivity/Convergence Analysis

Table 3: Mesh Sensitivity/Convergence Analysis Results

	No of Nodes	No of Elements	Max Temperature	Approx Element Size
Mesh 0	254	28	57.9588	70
Mesh 1	348	40	57.8918	65
Mesh 2	348	40	57.8918	60
Mesh 3	388	45	57.9163	55
Mesh 4	503	60	57.9987	50
Mesh 5	632	77	58.0007	45
Mesh 6	836	104	58.0144	40
Mesh 7	1000	126	58.0032	35
Mesh 8	2901	340	55.2353	30
Mesh 9	2901	480	55.0803	25
Mesh 10	6072	1125	53.6345	20
Mesh 11	10490	1980	53.5437	15
Mesh 12	35871	7500	53.6704	10

Full-Scale Sidewalk Construction and Field Testing

A full-scale pilot sidewalk was constructed on the UTSA campus to validate the laboratory and modeling findings under outdoor conditions. The test section consists of six adjacent 4 ft × 4 ft sidewalk segments **(Figure 10)**, each 3 in. thick, placed over a common base and subbase and exposed to identical environmental conditions. For the field implementation, only the sand-replacement PCM method was used. The addition method was intentionally excluded for two practical reasons:

1) Material quantity and cost: when scaled up to field construction, the addition method requires a significantly larger mass of PCM per panel because it does not replace any constituent (it is added on top of the existing mix), which would make sidewalk production substantially more expensive.
2) Mechanical trade-offs: mechanical testing showed a clearer negative impact on compressive strength and workability for the addition method compared with sand-replacement at similar

PCM percentages, since no aggregate or paste is removed to compensate for the added PCM. Given these trade-offs and the TxDOT sidewalk performance criteria, the addition method was not selected for field construction.

The six segments implement different cooling mechanisms **(Figure 11):**

1) Conventional concrete control segment.
2) 5% PCM concrete segment using the sand-replacement method.
3) Sand-blasted concrete segment without PCM.
4) 2.5% PCM concrete with surface sand-blasting treatment.
5) Diamond-grinded concrete segment without PCM.
6) 2.5% PCM concrete with a diamond-grinded surface.

All segments were cast in place in wooden forms set at the test location, using the optimized sand-replacement concrete mixes that met strength and workability requirements relative to TxDOT sidewalk specifications. After curing, sand-blasting, and diamond-grinding were applied to the designated segments to increase surface albedo and modify surface texture. Thermal instrumentation consisted of embedded or surface-mounted thermocouples connected to a portable thermocouple data logger positioned adjacent to the sidewalk. Each segment was instrumented at representative locations along the centerline. For each monitoring week, temperature data were collected continuously from 10:00 p.m. on the first day to 10:00 p.m. on the seventh day, providing a full seven-day thermal profile for all six segments. This weekly monitoring protocol has been applied over approximately three consecutive months and remains ongoing to capture seasonal variation and aging effects. Surface temperature time series are processed at 5-minute intervals, and weekly profiles are compared among the six segments to quantify the relative temperature reduction achieved by (a) PCM integration alone, (b) surface treatments alone, and (c) combining PCM plus surface-treatment strategies. The field measurements are used to validate and refine the FE model predictions and to develop practical guidelines for specifying PCM content and surface treatments in precast sidewalks intended for UHI mitigation.

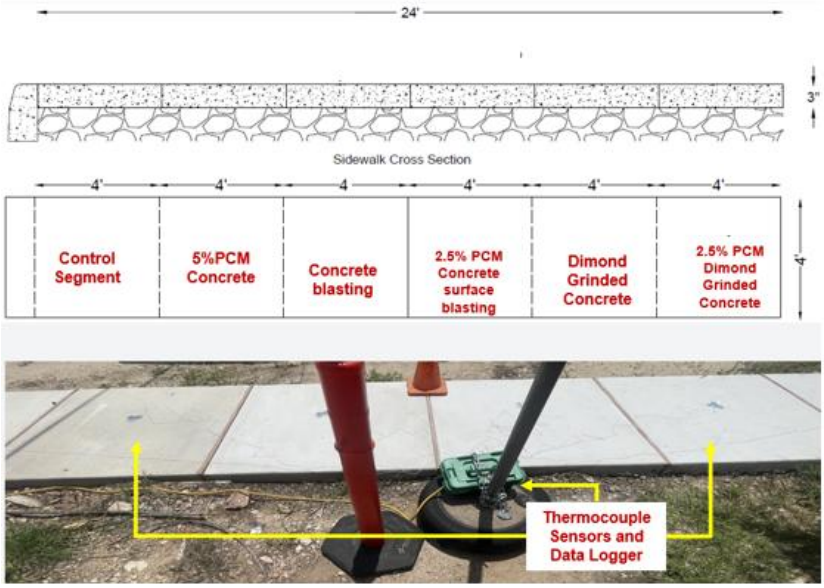

Figure 10: Design and Construction of a Cool Sidewalk with Different Cooling Mechanisms

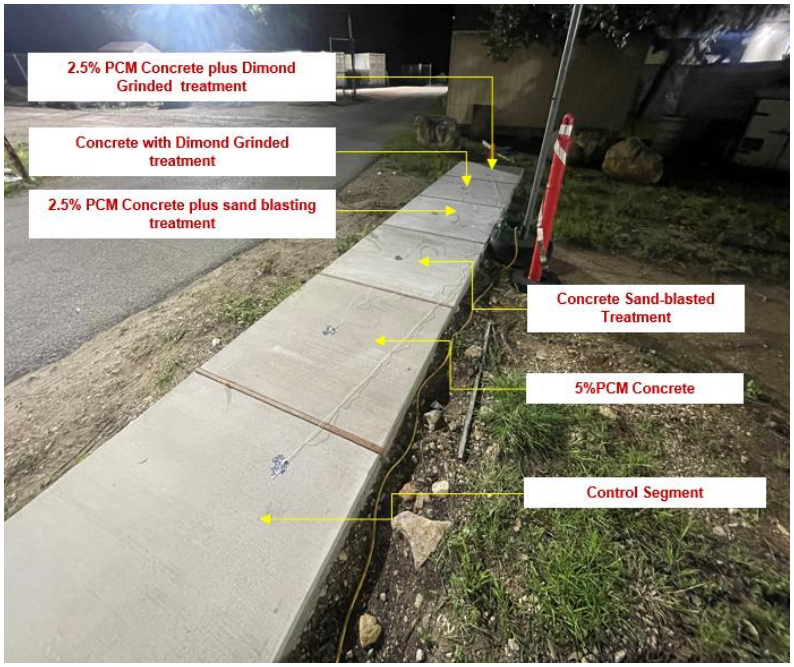

Figure 11: Full Scale Test of Different Cooling Mechanisms

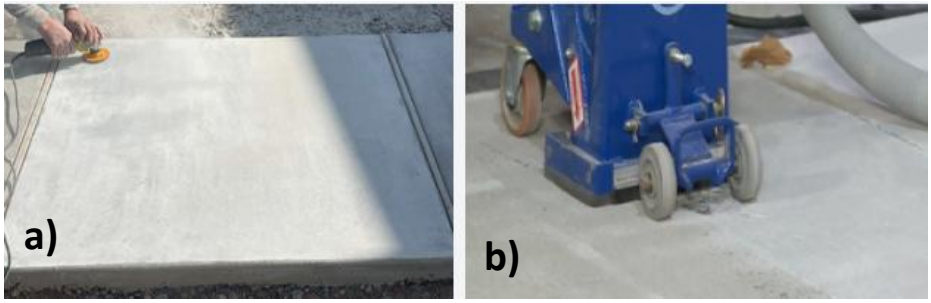

Figure 12: Two Surface Albedo Enhancement; a) Dimond Grinding b) Sand Blasting

In summary, the methodology combines material-level mechanical testing, advanced thermal finite element modeling, and full-scale field experimentation into a unified framework for assessing PCM-enhanced precast sidewalks. The mechanical phase establishes which PCM dosages and integration methods meet TxDOT-type sidewalk performance criteria. The FE modeling phase extends the laboratory findings by simulating realistic thermal boundary conditions and exploring alternative design scenarios. The full-scale pilot sidewalk links these elements under real weather exposure, enabling direct comparison of different PCM and surface-treatment configurations and supplying the data needed to validate and refine the numerical model. Together, these methods provide a robust basis for evaluating PCM-integrated precast sidewalks as a practical cool pavement solution.

CHAPTER 4: RESULTS AND ANAYLSIS

Mechanical Properties – Compressive Strength and Workability

Figure 14 presents the average 7-, 14-, and 28-day compressive strengths for the control concrete and the PCM-modified mixes, together with the TxDOT design requirement of 3000 psi minimum 28-day strength for general-use sidewalk concrete (w/c = 0.60) **(Figure 13).** All mixes were tested

using three 4 in. × 8 in. cylinders per age, and the error bars represent the standard deviation of the three replicates. Slump values measured at the time of casting are summarized in Table 4. At all ages, the control mix (0% PCM) exhibited the highest compressive strength, reaching approximately 6000 psi at 28 days, which is well above the TxDOT design requirement. The 5% PCM sand-replacement mix (5% R-PCM) showed a reduction in strength relative to the control but still developed a 28-day strength on the order of three-quarters of the control value and above the 3000-psi design limit. The higher PCM level in the sand-replacement mix (10% R-PCM) led to a more pronounced loss of strength; its 28-day strength remained well below the control and below the TxDOT design value, indicating that 10% replacement is not suitable for structural sidewalk applications. For the addition method, both 5% A-PCM and 10% A-PCM mixtures exhibited lower compressive strengths than the control across all ages. While the 5% addition mix showed some strength gain with age, its 28-day strength was still substantially below the control and close to or below the TxDOT design target, and the 10% addition mix remained significantly weaker. These trends confirm that increasing PCM content beyond about 5% leads to diminishing mechanical performance, regardless of the integration method. Workability results follow the same pattern. The control mix had a slump of 3.4 in., within the TxDOT general-usage slump range of 3–5 in. Both sand-replacement mixes preserved acceptable workability, with slumps of 3.3 in. (5% R-PCM) and 3.1 in. (10% R-PCM). In contrast, PCM addition resulted in a marked reduction in slump: 2.1 in. for 5% A-PCM and 1.3 in. for 10% A-PCM, both falling below the TxDOT recommended slump range and indicating a much stiffer, less workable mixture as shown in **Table 4.**

Concrete Class on Plans:	
General Usage (Note 1):	
Design Strength, Min. 28-day f'c (psi):	3000
Specified Design Strength, Min. 28-day f'c (psi):	
Max. W/C Ratio:	0.60
Optimized Gradation Design?:	

Acceptable Coarse Aggregate Grades:	Grade 8
Acceptable Cement Types:	Type I/II
Available Mix Design Options:	1
Acceptable Slump Range:	Choose a General Usage
Design Slump Range:	3"-5"

Mix Design Input:	Existing design

Figure 13: Texas Department of Transportation's Design Requirements for a Curbside or A Sidewalk Design [90].

Overall, the mechanical study shows that:

- PCM integration inevitably reduces compressive strength compared with the control mix, with the reduction increasing as PCM content increases.
- Among the mixes tested, 5% PCM using the sand-replacement method offers the best balance between mechanical performance and PCM content: it meets the TxDOT 28-day strength requirement and maintains slump within the target range.
- The addition method produces larger losses in workability and strength for the same PCM percentage and would require significantly more PCM at field scale, making it less attractive for practical sidewalk construction. These results motivated the choice of sand-replacement PCM mixes, particularly around the 5% level, for subsequent finite element modeling and for the full-scale cool sidewalk implementation.

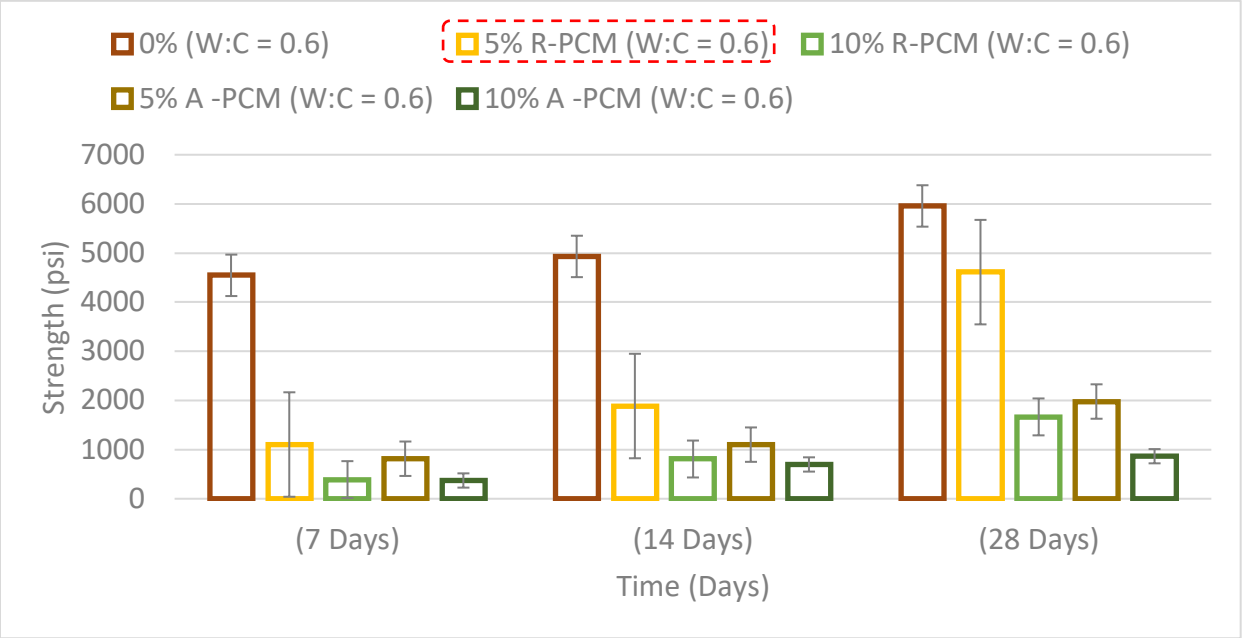

Figure 14: Mechanical Compressive Strength for The Two Methods Addition and Sand Replacement Of PCM

Table 4: Slump Test for Workability

Sample ID	Slump
0% PCM (W:C = 0.6)	3.4
5% R-PCM (W:C = 0.6)	3.3
10% R-PCM (W:C = 0.6)	3.1
5% A -PCM (W:C = 0.6)	2.1
10% A -PCM (W:C = 0.6)	1.3

Finite Element Modelling Results

To complement the laboratory thermal experiments, a three-dimensional transient finite element (FE) model was developed in ABAQUS to simulate the temperature response of the concrete slabs under controlled heating–cooling cycles as shown in **Figure 15**. The model incorporated the measured thermal properties of the control and PCM-modified concretes and replicated the test configuration of the insulated chamber, including radiation from the heat lamps and natural convection inside the box. Separate material definitions were used for each PCM dosage and integration method (addition and sand replacement), allowing the effects of increased heat capacity and reduced thermal conductivity to be represented explicitly in the analysis. The FE simulations were performed for both 4-hour (2 hr. heating + 2 hr. cooling) and 8-hour (4 hr. heating + 4 hr. cooling) cycles. For each case, nodal temperatures corresponding to the locations of the top and bottom thermocouples were extracted and compared directly with the experimental measurements. Model performance was quantified using the RMSE between simulated and measured temperatures. The following subsections present the results for each PCM content and mixing method and assess how well the calibrated model reproduces the observed thermal behavior and the cooling benefits associated with PCM integration.

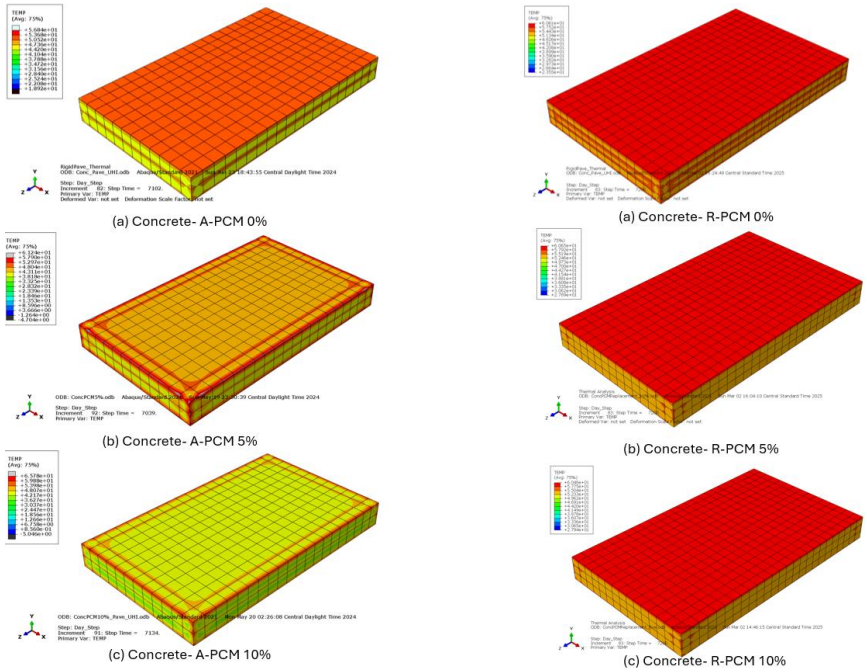

Figure 15: Six Finite Element Models for the Two Methods the addition and the Sand Replacement of PCM

Four-hour heating–cooling cycle – Addition method (A-PCM)

Figure 16 shows the comparison between experimental and finite element (FE) temperatures at the top and bottom surfaces of the slab for the 4-hour cycle using the addition method (0%, 5%, and 10% A-PCM). For the control mix (0% A-PCM), the FE model reproduced both the heating and cooling curves with good agreement; the RMSE values between measured and simulated temperatures were about 1.0 °C for the top and 2.0 °C for the bottom during heating and remained close to 1–1.5 °C during the cooling stage. The model captured the continuous increase in surface temperature from roughly the mid-20s to the mid-40s °C and the slightly delayed response at the bottom surface. For the 5% A-PCM slab, the model again followed the experimental trend, with RMSE values on the order of 0.8 °C for the top and 2.6 °C for the bottom in the heating phase. The curves show that the presence of PCM reduced the rate of temperature rise and slightly lowered the peak temperature at the top surface compared with the control slab. During cooling, the FE and experimental curves almost overlapped, with RMSE values close to 1 °C for both surfaces, indicating that the model was able to capture the delayed cooling response associated with the latent heat release of PCM. The 10% A-PCM slab exhibited the strongest latent-heat effect. The FE results matched the experimental curves with RMSE values of about 0.7 °C (top) and 0.6 °C (bottom) in heating, and around 0.4–1.1 °C in cooling. The temperature rise at the top surface was noticeably flatter, and the overall peak temperature was several degrees lower than the control. The bottom surface remained cooler than the top throughout the cycle, with the gap narrowing during the cooling phase as heat diffused through the slab. Overall, the 4-hour simulations for the addition method show that the calibrated model reproduces the measured thermal histories with errors generally below ±2 °C and clearly reflects the reduction in peak temperature and the smoothing of the temperature curve as PCM content increases.

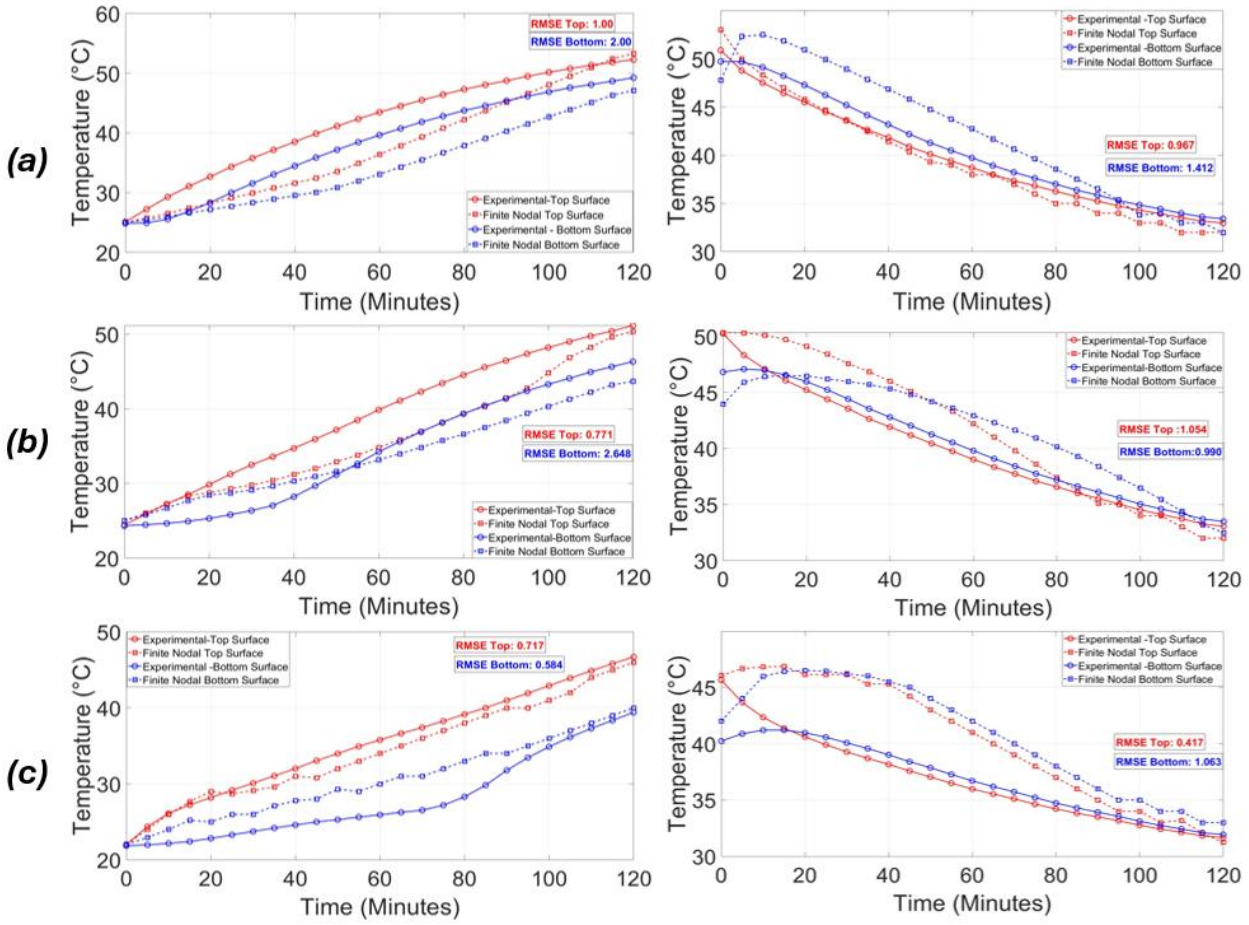

Figure 16: Four-hour heating–cooling cycle – Addition method (A-PCM); a) 0% A-PCM, b) 5% A-PCM, c) 10% A-PCM

Four-hour heating–cooling cycle – Sand-replacement method (R-PCM)

Figure 17 presents the same 4-hour cycle comparison for the sand-replacement method (0%, 5%, and 10% R-PCM). For the 0% R-PCM control slab, the FE predictions closely tracked the experimental heating curve, with RMSE values of about 1.0 °C for the top and 1.1 °C for the bottom surfaces. During the cooling period, the agreement remained good, with RMSE values around 1.0 °C for both surfaces. The model correctly reproduced the approximately linear temperature rise to the mid-50s °C and the gradual decrease during cooling. For the 5% R-PCM slab, the model predicted slightly lower heating and cooling curves relative to the control, in line with the experimental data. The RMSE values were approximately 0.7 °C (top) and 0.8 °C (bottom) during heating and about 1.0 °C in cooling, showing very good agreement. The top-surface temperature rose more slowly and reached a slightly lower peak, while the bottom surface showed an even smaller increase, indicating that the sand-replacement PCM also provided a modest reduction in through-thickness temperature. In the 10% R-PCM slab, the FE model continued to perform well, with RMSE values of approximately 1.1 °C (top) and 1.0 °C (bottom) for the heating period and about 0.9–1.0 °C for cooling. The effect of PCM was visible as a further reduction in the heating rate and a modest drop in peak temperature compared with the 0% case. Overall, the 4-hour R-PCM simulations confirm that the model represents both integration

methods consistently and can capture the relatively smaller but still noticeable cooling benefit obtained with sand-replacement PCM.

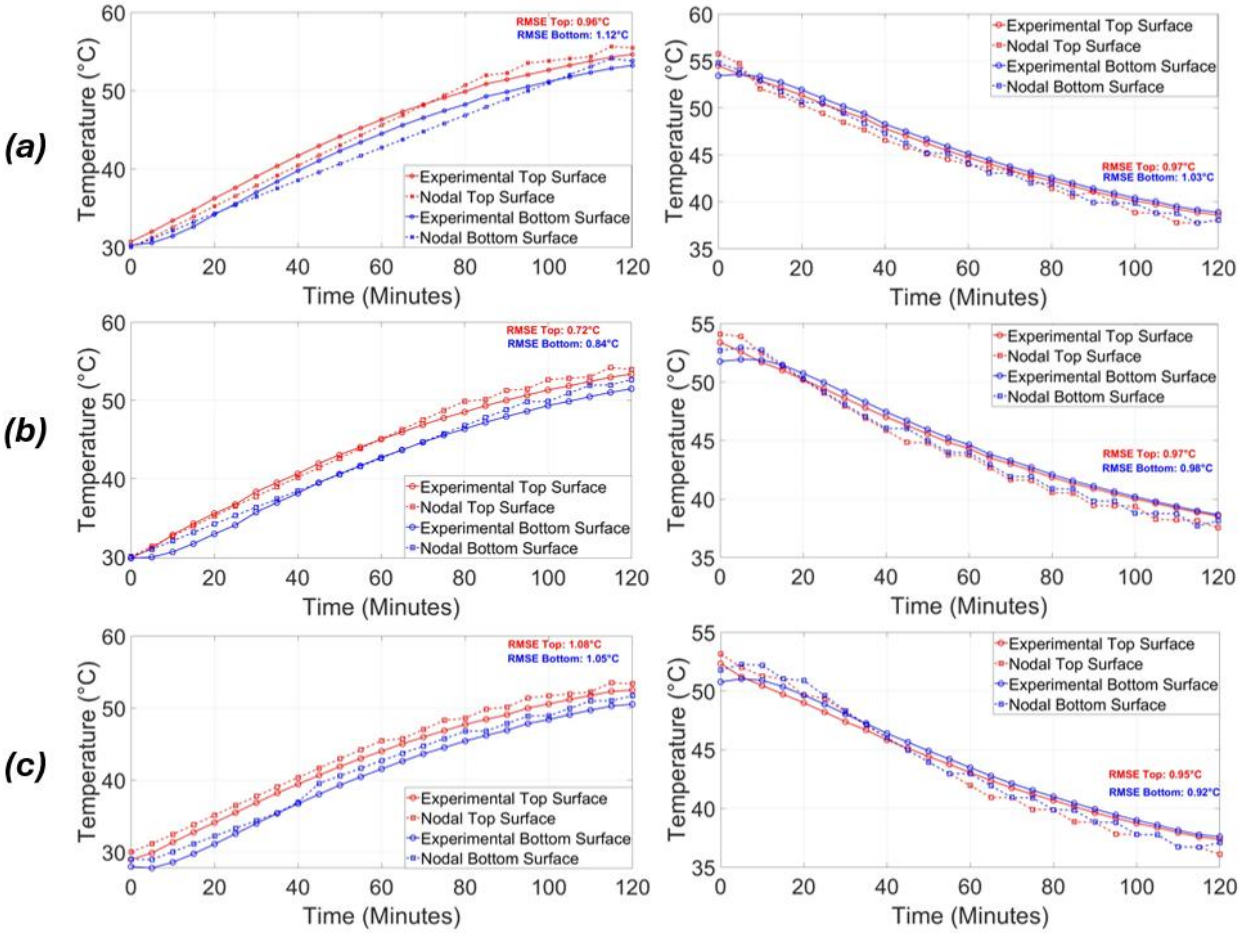

Figure 17: Four-hour heating–cooling cycle – Sand Replacement method (R-PCM); a) 0% A-PCM, b) 5% R-PCM, c) 10% R-PCM

Eight-hour heating–cooling cycle – Addition method (A-PCM)

Figure 18 compares the FE and experimental temperature histories for the 8-hour cycle (4 hr. heating + 4 hr. cooling) for the addition method, highlighting model performance under extended heating and partial thermal saturation. For the 0% A-PCM control slab, the FE curves closely matched the experimental data, with RMSE values of about 1.0 °C at both the top and bottom surfaces in both heating and cooling. The top surface warmed from roughly 30 °C to the mid-60s °C, while the bottom surface remained several degrees cooler, indicating a through-thickness gradient. With 5% A-PCM, the temperature rose more slowly and reached a slightly lower peak than the control; the model reproduced this behavior with RMSE values of about 1.6 °C (top) and 1.5 °C (bottom) during heating, and about 1.4 °C (top) and 0.9 °C (bottom) during cooling. For the 10% A-PCM slab, the latent-heat effect is more evident: the heating curve flattens, and the peak temperature is further reduced. The model captured these trends with RMSE values of about 1.5 °C (top) and 2.0 °C (bottom) in heating and roughly 0.9–1.1 °C in cooling. These results

confirm that the FE model remains reliable over longer cycles and reflects the increased thermal storage and reduced peak temperatures with higher PCM content.

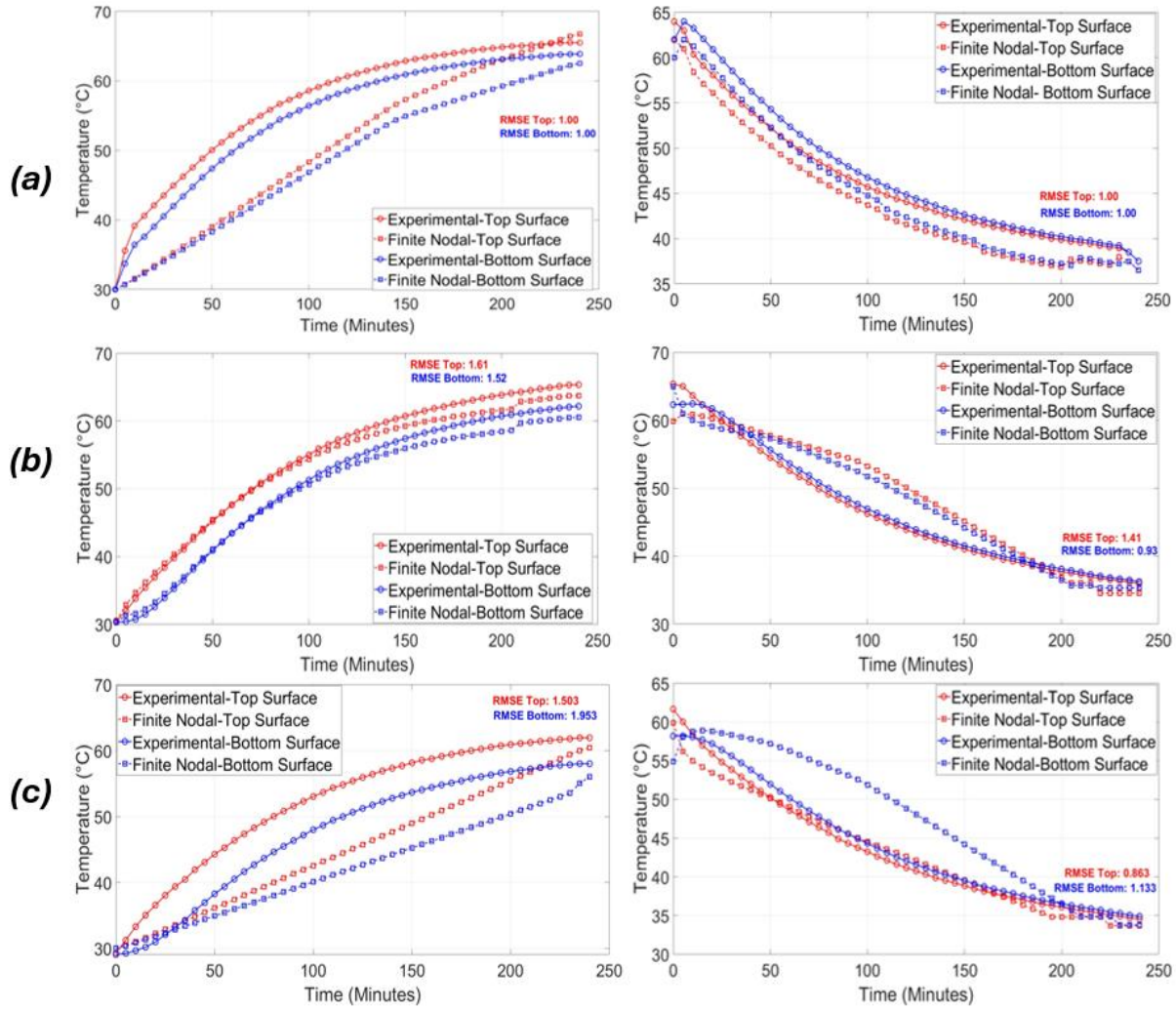

Figure 18: Eight-hour heating–cooling cycle – Addition method (A-PCM); a) 0% A-PCM, b) 5% A-PCM, c) 10% A-PCM

Eight-Hour Heating–Cooling Cycle – Sand-Replacement Method (R-PCM)

Figure 19 shows the 8-hour cycle results for the sand-replacement method. For the 0% R-PCM control slab, the FE model predicted the temperature histories with RMSE values of about 1.8 °C (top) and 1.4 °C (bottom) during heating and roughly 0.8–1.1 °C during cooling. The heating curve again rose from the low-30s to around 60 °C at the top surface, with a smaller increase at the bottom. The 5% R-PCM slab showed a noticeable reduction in heating rate and a modest drop in peak surface temperature relative to the control. The FE model reproduced this behavior with improved accuracy compared with the 0% case: RMSE values were approximately 0.7 °C for the top and 1.2 °C for the bottom surfaces in heating and about 0.6–1.3 °C during cooling. The model captured both the delayed heating due to PCM melting and the slightly slower cooling associated with latent-heat release. For the 10% R-PCM slab, the experimental data indicated additional smoothing of the temperature curve, although the peak temperature reduction was smaller than

that observed for the addition method at the same PCM content. The FE predictions followed the overall trend, with RMSE values on the order of 1.0 °C (top) and 2.0 °C (bottom) during heating and about 0.9–1.3 °C in cooling. Despite slightly larger deviations at the bottom surface near the end of the heating period, the model still captured the essential features of the thermal response.

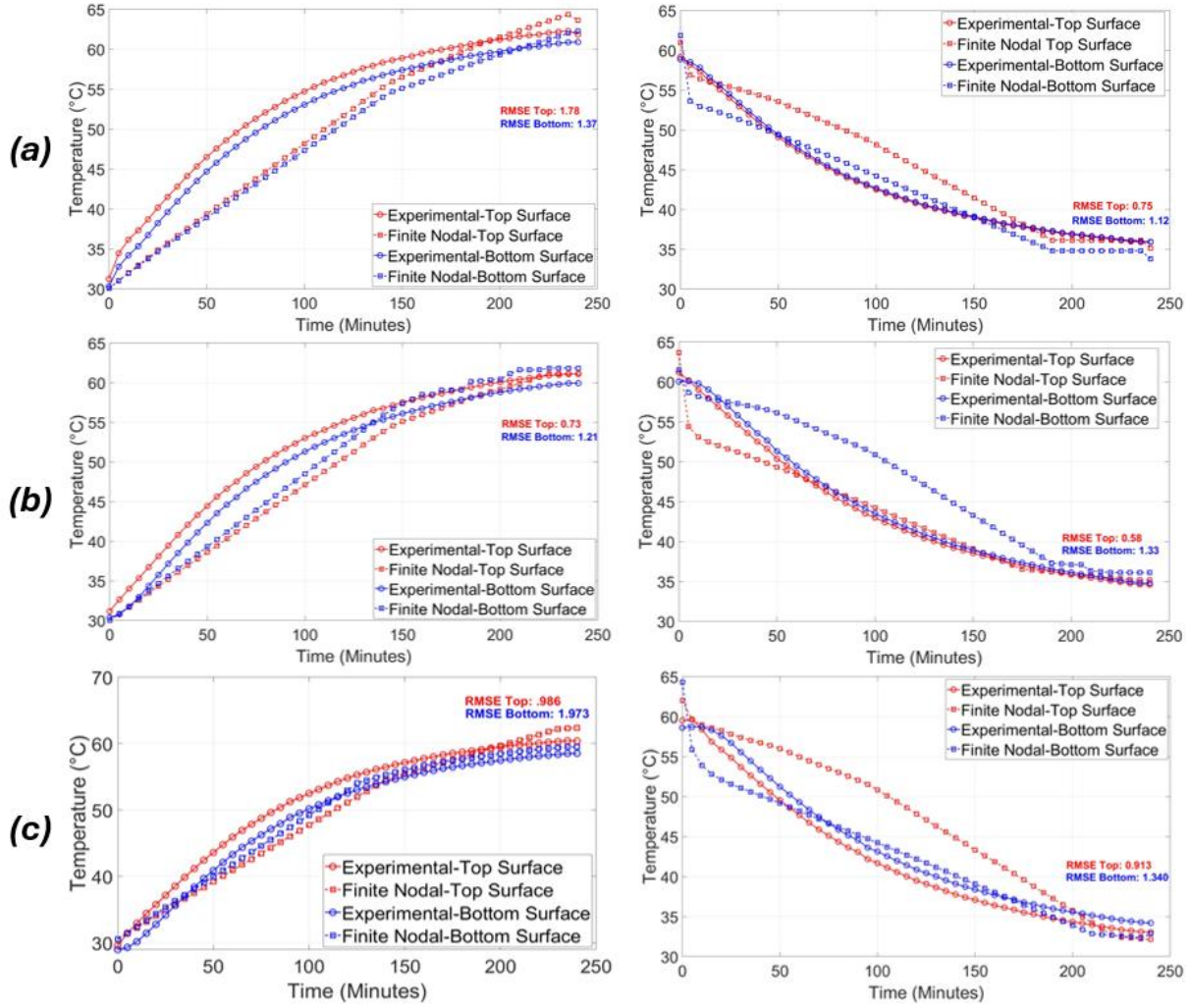

Figure 19:Eight-hour heating–cooling cycle – Sand Replacement method (R-PCM); a) 0% A-PCM, b) 5% R-PCM, c) 10% R-PCM

Summary of FE performance

Across all PCM contents, integration methods, and cycle durations, the calibrated FE model reproduced the measured top and bottom surface temperatures with RMSE values generally below 2 °C, which is acceptable for pavement-scale thermal analysis. The simulations clearly showed increasing PCM content:

- Reduces the rate of temperature increase and lowers peak surface temperatures, particularly for the 10% A-PCM case.
- Narrows the temperature gradient between top and bottom surfaces during the cooling phase, reflecting increased heat storage and delayed release.

- Produces similar qualitative behavior for both the addition and sand-replacement methods, with the addition method showing somewhat stronger temperature reductions for the same PCM percentage.

These FE results provide confidence that the model can be used to extrapolate beyond the tested conditions, evaluate different PCM dosages and slab geometries, and support the design of PCM-enhanced precast pavements for UHI mitigation.

Full-Scale Sidewalk Test – Experimental Setup

A full-scale pilot sidewalk was constructed on the University of Texas at San Antonio campus to evaluate the in-service thermal performance of PCM-enhanced concrete and surface treatments under outdoor conditions. The test section consists of six adjacent 1.22 m × 1.22 m (4 ft × 4 ft) sidewalk panels, each 76 mm (3 in.) thick, cast over a common compacted base so that all panels experience essentially identical solar radiation and ambient weather. All concrete mixes were proportioned using the same control mixture as a baseline; PCM was incorporated only through the sand-replacement method to avoid the high material demand and mechanical penalties associated with the addition method at field scale. The six panels represent distinct combinations of PCM dosage and surface treatment. The control concrete segment consists of conventional concrete with no PCM and no surface treatment. The 5% PCM concrete segment contains 5% PCM by weight of the control mix, replacing a portion of the fine aggregate, and has no surface treatment. The sand-blasted segment is made from the control concrete, but its surface is sand-blasted to increase roughness and effective albedo. The sand-blasted Plus 2.5% PCM segment combines a 2.5% PCM sand-replacement mix with the same sand-blasted surface treatment. The diamond-grinded segment consists of control concrete with a diamond-grinded surface, while the diamond-grinded plus 2.5% PCM segment combines the 2.5% PCM mix with a diamond-grinded surface. Surface temperatures of each panel were monitored using thermocouples mounted on the slab surface and connected to a multi-channel thermocouple data logger placed adjacent to the sidewalk. Data was recorded at 10-minute intervals. For analysis, temperatures were first averaged over each week (seven-day mean profile for each time of day), and then weekly profiles were averaged to obtain a representative monthly diurnal profile for each segment. **Figures 20–22** present these monthly average profiles for the first, second, and third monitoring months, together with the corresponding monthly maximum and minimum ambient air temperatures.

Monthly Cooling Benefit Index (MCBI)

Because each panel yields a full 24-hour temperature history for every week and month, direct visual comparison of all curves does not provide an efficient or quantitative means of ranking performance. To condense the data into a single, physically meaningful indicator, a MCBI was defined. The index focuses on the afternoon period when UHI impacts, pedestrian exposure, and pavement cooling demands are most critical. In this study, the hot-period window was taken as 12:00–10:00 p.m., corresponding to Time = 840–1440 minutes in the data set. For each segment $s$and month m, the mean afternoon surface temperature is computed as

$$\bar{T}_{s,m} = \frac{1}{N} \sum_{t \in (12:00–22:00)} T_{s,m}(t) \qquad Eq.\,(1)$$

where $T_{s,m}(t)$is the surface temperature of segment s at time t, and N is the number of time steps within the afternoon window. The corresponding mean afternoon temperature of the control segment in month m is

$$\bar{T}_{\text{control},m} = \frac{1}{N} \sum_{t \in (12:00–22:00)} T_{\text{control},m}(t) \qquad Eq.(2)$$

The MCBI is then defined as

$$\text{MCBI}_{s,m} = \bar{T}_{\text{control},m} - \bar{T}_{s,m} \qquad Eq.(3)$$

By construction, a positive $\text{MCBI}_{s,m}$indicates that segment $s$is cooler than the control on average during the critical afternoon period, a value of zero indicates similar behavior to the control, and a negative value indicates that the segment is warmer than the control. Expressing the index directly in degrees Celsius makes it easy to interpret as the average afternoon temperature reduction (or increase) relative to conventional concrete while also compressing the diurnal and multi-day data into a compact matrix that can be visualized using a heatmap**.**

RESULTS

The monthly diurnal profiles in **Figures 20–22** show that all six segments follow the same general pattern as the ambient air temperature, with minimum surface temperatures occurring near sunrise and peak values between approximately 4:00 p.m. and 6:00 p.m**.** The first month corresponds to the highest ambient maxima and produces the largest surface temperatures, whereas the second and third months are slightly cooler overall. Within each month, however, the relative ordering of the segment curves is not always obvious by visual inspection, which motivates the use of MCBI to compare configurations.

The computed MCBI values are summarized in the matrix in **Table 5**. During the first month, the 5% PCM concrete segment exhibited an MCBI of –1.95 °C, indicating that it was on average nearly 2 °C warmer than the control during the afternoon window. The sand-blasted and diamond-grinded segments were also slightly warmer than the control, with MCBI values of –0.50 °C and –0.63 °C, respectively. Only the sand-blasted plus 2.5% PCM segment provided a small cooling benefit, with an MCBI of +0.14 °C, while the diamond-grinded Plus 2.5% PCM configuration was essentially neutral (–0.22 °C). These results show that, under the hottest conditions, PCM at a 5% dosage without surface treatment does not reduce surface temperatures in the field and can in fact increase them relative to conventional concrete. In the second month, the performance of the surface-treated segments improved. The sand-blasted segment became marginally cooler than the control, with an MCBI of +0.07 °C, while the sand-blasted plus 2.5% PCM segment achieved a more pronounced mean afternoon reduction of +0.33 °C. In contrast, both diamond-grinded configurations remained warmer than the control, with MCBI values of –0.97 °C for the diamond-grinded segment and –1.30 °C for the diamond-grinded plus 2.5% PCM segment. The 5% PCM segment continued to exhibit a negative MCBI (–0.75 °C), confirming that PCM alone at this dosage is not an effective cooling strategy in the outdoor sidewalk application. By the third month, the beneficial effect of combining surface texturing with modest PCM content became much clearer. The sand-blasted concrete segment without PCM produced the largest cooling benefit, with an MCBI of +1.95 °C, indicating that it reduced the average afternoon surface temperature by nearly 2 °C compared with the control. The sand-blasted plus 2.5% PCM segment also performed very well, with an MCBI of +1.71 °C. The diamond-grinded segment became

moderately cooler than the control, with an MCBI of +0.61 °C, whereas the diamond-grinded plus 2.5% PCM segment remained close to neutral, with an MCBI of –0.08 °C. The 5% PCM segment, which had been consistently warmer than the control in the first two months, showed a slight improvement in the third month with an MCBI of +0.30 °C, but its performance still lagged behind the sand-blasted configurations.

The full-scale results indicate that PCM incorporated at 5% by sand replacement without any surface modification does not provide a robust cooling benefit under the tested climatic conditions and can increase surface temperatures during the hottest periods. In contrast, surface treatments play a dominant role in controlling sidewalk surface temperature. Sand-blasting, in particular, produced consistent and substantial reductions in mean afternoon temperature, and the combination of sandblasting with 2.5% PCM yielded a configuration that maintained adequate mechanical performance while delivering up to approximately 1.7–1.95 °C of cooling relative to the control. Diamond-grinding provided more modest and less consistent improvements and pairing it with 2.5% PCM did not outperform the sand-blasted options. The MCBI framework therefore provides a concise and interpretable tool for ranking full-scale sidewalk configurations and supports the conclusion that sand-blasted surfaces with modest PCM contents are the most promising strategy for practical cool-sidewalk implementation in this field setting.

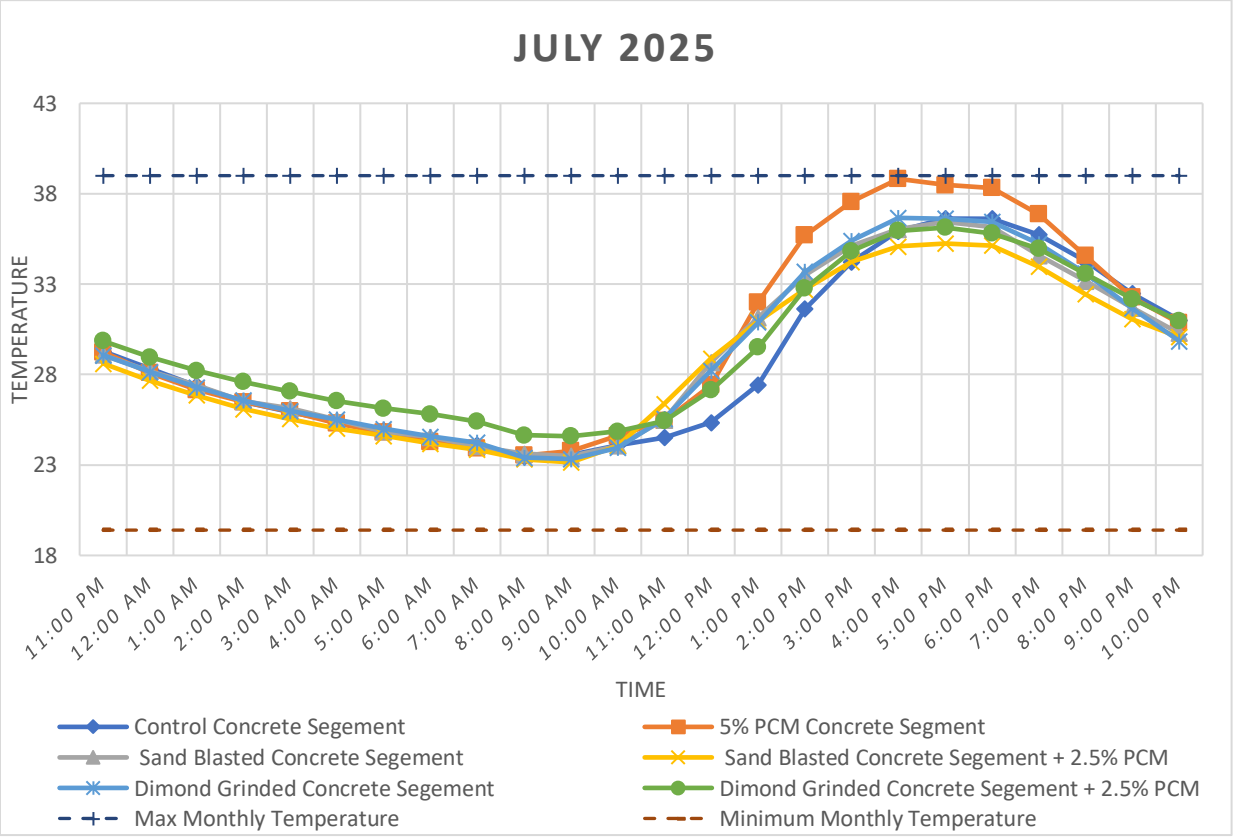

Figure 20: Full-Scale Sidewalk Test –July 2025 Monthly Results

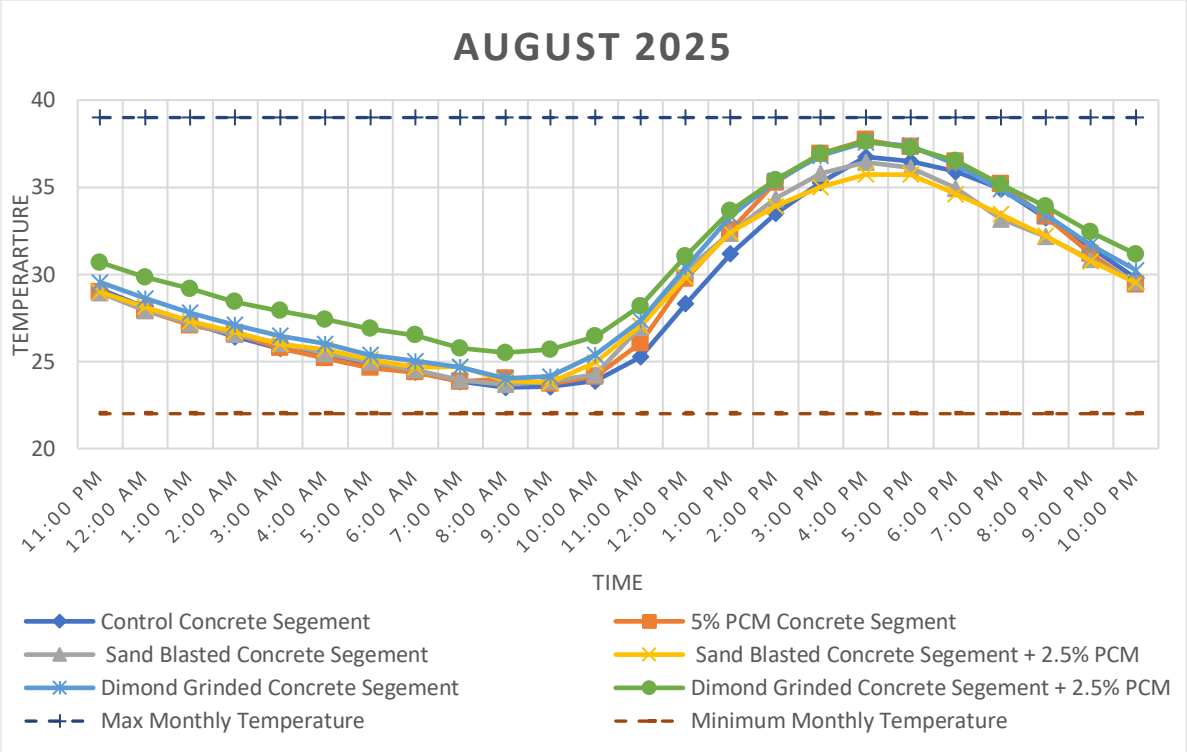

Figure 21: Full-Scale Sidewalk Test –August 2025 Monthly Results

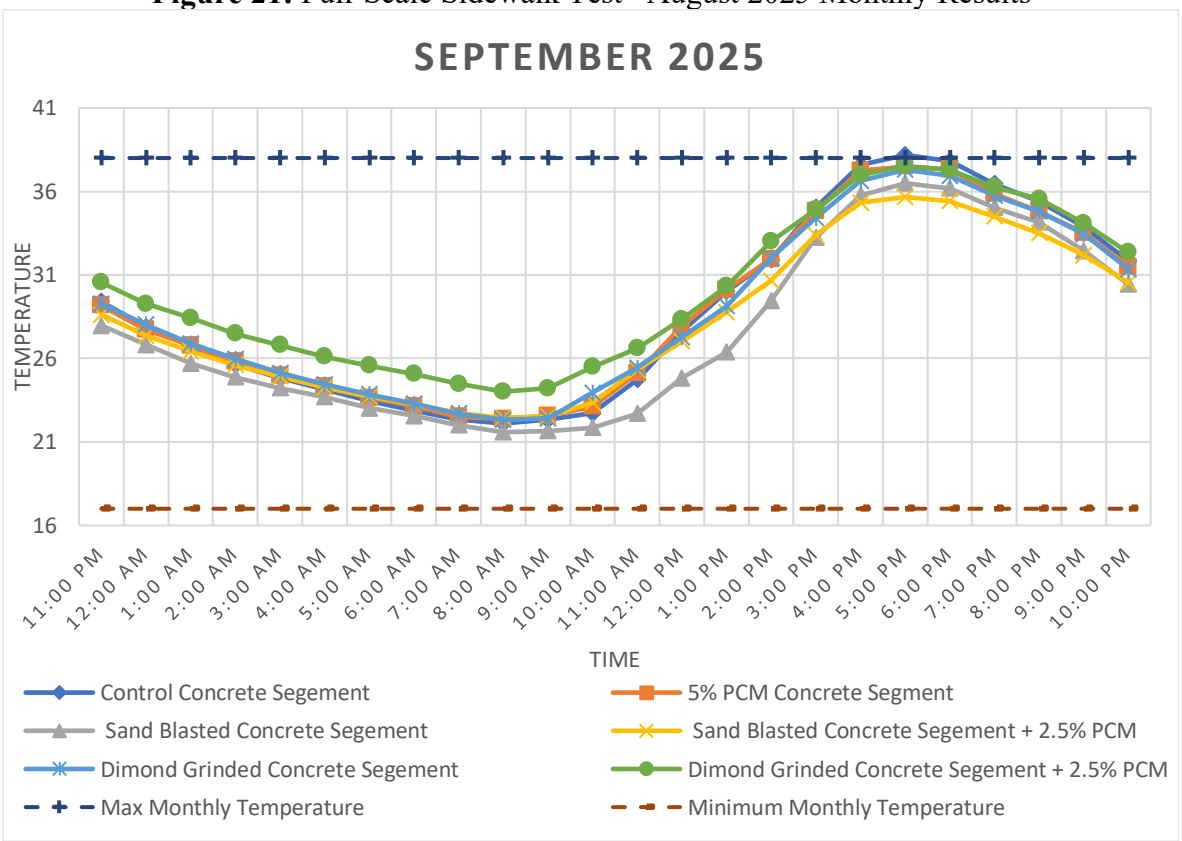

Figure 22: Full-Scale Sidewalk Test –September 2025 Monthly Results

Table 5: Heat-Map of Monthly Cooling Benefit Indices

Cooling Effect (Heating → Cooling)	MCBI 1st Month	MCBI 2nd Month	MCBI 3rd Month
Control Concrete	0.00	0.00	0.00
5% PCM Concrete	-1.95	-0.75	0.30
Sand Blasted Surface Concrete	-0.50	0.07	1.95
Sand Blasted-2.5% PCM Concrete	0.14	0.33	1.71
Dimond Grinded Surface Concrete	-0.63	-0.97	0.61
Dimond Grinded-2.5% PCM Concrete	-0.22	-1.30	-0.08

CHAPTER 5: CONCLUSIONS AND RECOMMENDATIONS

Mechanical Performance and Constructability

Mechanical testing revealed a clear trade-off between thermal enhancement and structural performance. Compressive strength and slump test results for the different PCM mixtures were evaluated against the TxDOT design specification for sidewalk concrete, which requires a minimum 28-day compressive strength of 3000 psi and a target slump in the range of 3–5 in. The control mix comfortably exceeded these requirements, reaching a 28-day compressive strength on the order of 6,000 psi, roughly twice the design value, with a slump of 3.4 in. For the sand-replacement (R-PCM) mixtures, 5% and 10% PCM both showed reduced strength relative to the control but still maintained acceptable performance. At 28 days, the 5% R-PCM mix achieved a strength above the 3000-psi design threshold, and the 10% R-PCM mix remained only moderately lower. Workability was only slightly affected: slump decreased from 3.4 in for the control to 3.3 in for 5% R-PCM and 3.1 in for 10% R-PCM, remaining within or very close to the TxDOT target range. These results indicate that sand replacement at 5–10% PCM can be used in sidewalk-strength concrete without compromising constructability and with only a modest loss in strength. In contrast, the addition (A-PCM) mixtures showed a more pronounced penalty. Because PCM is added on top of the base mix without replacing any constituents, the total paste volume and admixture demand increase, which aggravated both strength and workability. The 5% A-PCM mix still reached an acceptable 28-day strength but with a larger margin of reduction relative to the control, while the 10% A-PCM mixture exhibited a substantial strength drop and approached the lower bound of structural acceptability. Slump values reflected this trend: they dropped from 3.4 in (control) to 2.1 in for 5% A-PCM and 1.3 in for 10% A-PCM, moving well below the preferred 3–5 in range and signaling potential placement and finishing difficulties in the field. Taken together, these results show that increasing PCM content especially through the addition method generally reduces both strength and workability compared with the control mix. Because the addition method does not replace conventional constituents, it requires a larger PCM quantity, increases material cost, and introduces a clearer strength and workability penalty. By comparison, the sand-replacement method at lower dosages (approximately 2.5–5% PCM by weight of the control mix) provides a more balanced compromise, offering thermal benefits while remaining compatible with sidewalk-strength concrete and practical batching and placement procedures. For

these reasons, the addition method was not adopted for the full-scale construction phase; instead, 2.5% and 5% PCM by sand replacement were selected as more realistic and constructible options.

Finite Element Modelling Capability

The three-dimensional transient finite element (FE) model developed in this project successfully reproduced the measured thermal response of the indoor slabs for both the 4-hour and 8-hour heating–cooling cycles and for both PCM incorporation methods. The model used measured thermal properties for each mix namely, increased heat capacity and reduced thermal conductivity and diffusivity with higher PCM contents and applied boundary conditions representing radiation from the two 250-W bulbs and natural convection inside the insulated chamber. Model predictions were evaluated against experimental data at the top and bottom slab surfaces using the RMSE. Across all mixes and cycles, RMSE values for the Addition Method typically ranged between about 0.4 and 2.6 °C, while those for the Sand-Replacement Method were generally within 0.6–2.0 °C. For example, in the 4-hour addition cases, the RMSE at the slab surface was approximately 1.0 °C for the control and 0.8–1.1 °C for the PCM mixes, and in the 8-hour sand-replacement cases, RMSE values remained near 1 °C for both top and bottom surfaces. These low error magnitudes relative to peak temperatures of 50–65 °C indicate that the model captures the dominant heat transfer mechanisms and the influence of PCM on thermal inertia with good fidelity. This level of agreement suggests that the calibrated FE framework can be used as a predictive tool to explore conditions beyond those directly tested in the laboratory, including different PCM dosages, slab thicknesses, heating durations, and boundary conditions. The model thus provides a robust basis for parametric studies and for developing design guidance that explicitly accounts for the modified thermal inertia of PCM-enhanced concrete, particularly when extending the concept to other precast elements such as traffic barriers or larger sidewalk panels.

Full-Scale Sidewalk Performance

The full-scale sidewalk pilot constructed on the UTSA campus provided a critical assessment of PCM and surface treatments under outdoor conditions. Over three consecutive months, surface temperatures were recorded every 10 minutes and then averaged over each week and over the three-month period. The monthly average diurnal profiles showed that all segments followed the same general pattern as the ambient air temperature, with minimum surface temperatures near sunrise and peak values in the late afternoon (approximately 4:00–6:00 p.m.). To quantitatively compare configurations, a MCBI was defined as the difference between the control segment's mean afternoon temperature (12:00–10:00 p.m.) and the mean afternoon temperature of each segment. Positive MCBI values indicate a cooler surface relative to control, and negative values indicate a warmer surface. For the first (hottest) month, the 5% PCM concrete segment without surface treatment exhibited an MCBI of –1.95 °C, meaning that it was on average almost 2 °C warmer than the control during the afternoon window. The sand-blasted and diamond-grinded segments were also slightly warmer than the control, with MCBI values of –0.50 °C and –0.63 °C, respectively. Only the sand-blasted plus 2.5% PCM segment provided a small positive benefit (+0.14 °C), while the diamond-grinded plus 2.5% PCM segment remained essentially neutral (–0.22 °C). In the second month, performance improved slightly as ambient maximum decreased. The sand-blasted segment produced a marginal cooling benefit (MCBI = +0.07 °C), and the sand-blasted plus 2.5% PCM segment showed a more evident reduction (+0.33 °C). In contrast, the

diamond-grinded and diamond-grinded plus 2.5% PCM segments became substantially warmer than the control, with MCBI values of –0.97 °C and –1.30 °C, respectively, and the 5% PCM segment remained hotter (–0.75 °C). These results confirm that PCM alone at 5% dosage, even when introduced through sand replacement, does not guarantee cooler surfaces and may exacerbate heating under peak conditions. By the third month, the influence of surface treatment became dominant. The sand-blasted concrete segment achieved the largest cooling benefit with an MCBI of +1.95 °C, nearly 2 °C cooler than the control on average during the afternoon. The sand-blasted plus 2.5% PCM segment provided a similar advantage with an MCBI of +1.71 °C. The diamond-grinded segment became moderately cooler (+0.61 °C), whereas the diamond-grinded plus 2.5% PCM segment remained essentially neutral (–0.08 °C). The 5% PCM segment, which had been consistently warmer than the control in the first two months, finally achieved a slight positive benefit (+0.30 °C) but still underperformed relative to the surface-treated configurations. Overall, the full-scale results emphasize that surface condition is a dominant factor in controlling sidewalk surface temperature, and that combining modest PCM content with a high-albedo, textured surface (particularly sandblasting) is more effective than increasing PCM dosage alone. In the field, the best-performing configurations yielded up to approximately 2 °C reduction in average afternoon surface temperature compared with conventional concrete, a magnitude that is consistent with the shorter-term laboratory-slab tests and meaningful from a pedestrian thermal comfort perspective.

Recommendations and Limitations for Practice and Research

For near-term implementation, the results support the use of modest PCM dosages (≈2.5–5% by sand replacement) in conjunction with high-albedo surface treatments, rather than relying on high PCM contents or PCM alone. In sidewalk applications, municipal agencies and transportation departments should prioritize surface modifications such as sandblasting and consider supplementing them with low PCM contents in locations where additional thermal buffering is desired, such as heat-vulnerable pedestrian corridors, transit stops, or school routes. High-dosage PCM mixes produced by the addition method are not recommended for routine sidewalk construction due to their increased material cost, reduced compressive strength, and poor workability (slump as low as **1.3 in** at 10% A-PCM). Before large-scale adoption, agencies should incorporate PCM-enhanced, surface-treated precast panels into limited demonstration projects and evaluate performance jointly with life-cycle cost, constructability, and maintenance requirements.

Future research should extend the present findings in several directions. Long-term durability of PCM-enhanced and surface-treated concretes should be assessed through extended testing of shrinkage, cracking, abrasion, freeze–thaw resistance, and surface scaling under repeated mechanical and environmental loading. Additional field trials across different climatic regions and urban morphologies are needed to quantify performance under a broader range of ambient maxima (for example, daily peaks from **30–40 °C**) and shading conditions. The FE framework should be expanded to couple heat transfer with moisture transport and possible degradation mechanisms, and to simulate other precast elements such as traffic barriers or larger precast panels that may experience different heat-flux patterns. Additionally, Given the fact that all the design mixes that have been conducted through the research are without using any type of admixtures such as water reducers or fly-ash to increase the workability, such these additives can enhance the workability and the strength and at the same time leave a space for adding more PCM to take advantage of its thermal buffering properties. Finally, integrating the thermal modelling and field data with life-

cycle assessment and human-thermal-comfort metrics would allow agencies to compare PCM-enhanced sidewalks with alternative cool-pavement strategies on a consistent basis. Quantifying benefits in terms of reduced peak surface temperatures (up to **~8 °C** at the slab scale and **~2 °C** at the field scale), potential reductions in cooling energy demand, and associated emissions will help refine design recommendations for urban heat-island mitigation at the corridor and network scale.

While the findings from this study are promising, several limitations should be acknowledged. First, the use of organic microencapsulated PCM adds material and manufacturing costs relative to conventional sidewalk concrete, particularly because PCM is a specialty product and its supply chain for pavement applications is still emerging. Second, PCM-integrated concrete is relatively new to the pavement industry; contractors, inspectors, and agencies have limited experience with its batching, placement, finishing, and quality control, which may slow near-term adoption. Third, the long-term durability of the microcapsules under repeated thermal cycling, moisture exposure, and potential mechanical damage (for example during mixing or surface grinding) has not yet been fully quantified and may influence long-term performance. In addition, the full-scale field evaluation was conducted at a single site on the UTSA campus over approximately three summer months, so the results may not fully capture performance under different climates, traffic levels, or multi-year aging. Finally, more design Mixes and dosages must be applied and tested by integrating PCM with admixtures such as water reducers or fly ash to fully understand the potential Impact of it and overcome its limitation for the strength and workability.

Practical Application/Impact on National Transportation Infrastructure:

The cooling strategy demonstrated in this project, modest PCM dosages combined with high-albedo, textured precast concrete surfaces can be extended well beyond sidewalks. Because it relies on conventional concrete constituents, sand-replacement PCM dosing, and standard finishing techniques (sandblasting, diamond grinding), the same approach is compatible with precast and cast-in-place rigid pavements used on highways, bridge decks, and airport pavements. For example, PCM-enhanced, textured precast panels could be deployed in rapid-replacement applications such as urban freeway main lanes, high-occupancy vehicle lanes, toll facilities, and major bridge decks, where heat mitigation is desirable, but closures must be minimized. Similarly, airfield shoulders, aprons, and selected taxiway or gate areas constructed with PCM-integrated concrete could reduce pavement surface temperatures around aircraft servicing zones and high-occupancy apron areas without changing existing construction practices. At the network level, the technology is particularly powerful when applied continuously along a corridor rather than as isolated panels. Retrofitting an entire downtown sidewalk network, transit corridor, or multimodal street with PCM-enhanced, sand-blasted precast panels would create a connected “cool surface layer” along building frontages and transit access paths. The cumulative effect of cooler surfaces over several blocks or miles is expected to reduce heat storage at the ground plane, lower mean radiant temperatures experienced by pedestrians, and moderate near-surface thermal loading during the hottest hours of the day. The same principle applies to corridor-scale deployments on roads and bridges: a sequence of cool pavement segments along an urban arterial or elevated structure would collectively reduce the amount of solar energy absorbed and re-radiated into the urban canopy, complementing cool roofs, reflective roadway treatments, and urban greening. From an implementation standpoint, this approach fits into existing national transportation programs by using standard materials and construction workflows with targeted modifications to mix design

and surface finishing. Agencies could first deploy PCM-enhanced, high-albedo precast panels in priority zones downtown cores, transit hubs, school zones, vulnerable neighborhoods, critical bridge decks, or airport operating areas and then phase them into routine reconstruction and preservation projects as a standard detail. Over time, building out continuous cool corridors across sidewalks, highways, bridges, and select airfield pavements would support broader National goals for climate-resilient infrastructure, heat-health protection, and reduced cooling energy demand.

REFERENCES

[1] T. R. Oke, "The energetic basis of the urban heat island," *Quart J Royal Meteoro Soc*, vol. 108, no. 455, pp. 1–24, Jan. 1982, doi: 10.1002/qj.49710845502.

[2] Oke, T. R. (1988). *The urban energy balance*. *Progress in Physical Geography*, *12*(4), 471-508. https://doi.org/10.1177/030913338801200401

[3] A. J. Arnfield, "Two decades of urban climate research: a review of turbulence, exchanges of energy and water, and the urban heat island," *Int. J. Climatol.*, vol. 23, no. 1, pp. 1–26, Jan. 2003, doi: 10.1002/joc.859.

[4] K. S. Al-Jabri, A. W. Hago, A. S. Al-Nuaimi, and A. H. Al-Saidy, "Concrete blocks for thermal insulation in hot climate," *Cement and Concrete Research*, vol. 35, no. 8, pp. 1472–1479, Aug. 2005, doi: 10.1016/j.cemconres.2004.08.018.

[5] C. S. B. Grimmond and T. R. Oke, "Heat Storage in Urban Areas: Local-Scale Observations and Evaluation of a Simple Model," *J. Appl. Meteor.*, vol. 38, no. 7, pp. 922–940, Jul. 1999, doi: 10.1175/1520-0450(1999)038<0922:HSIUAL>2.0.CO;2.

[6] K. Fortuniak, "Numerical estimation of the effective albedo of an urban canyon," *Theor Appl Climatol*, vol. 91, no. 1–4, pp. 245–258, Feb. 2008, doi: 10.1007/s00704-007-0312-6.

[7] Y. Qin and J. E. Hiller, "Understanding pavement-surface energy balance and its implications on cool pavement development," *Energy and Buildings*, vol. 85, pp. 389–399, Dec. 2014, doi: 10.1016/j.enbuild.2014.09.076.

[8] K. Anandakumar, "A study on the partition of net radiation into heat #uxes on a dry asphalt surface," *Atmospheric Environment*, 1999.

[9] H. Akbari and L. S. Rose, "Characterizing the fabric of the urban environment: A case studyof Metropolitan Chicago, Illinois and Executive Summary," LBNL--49275, Oct. 2001. doi: 10.2172/900694.

[10] H. Akbari, L. S. Rose, and H. Taha, "Characterizing the Fabric of the Urban Environment: A Case Study of Sacramento, California," LBNL-44688, 764362, Dec. 1999. doi: 10.2172/764362.

[11] H. Li, "Evaluation of Cool Pavement Strategies for Heat Island Mitigation".

[12] H. Akbari, M. Pomerantz, and H. Taha, "Cool surfaces and shade trees to reduce energy use and improve air quality in urban areas," *Solar Energy*, vol. 70, no. 3, pp. 295–310, 2001, doi: 10.1016/S0038-092X(00)00089-X.

[13] L. Gartland, *Heat islands: understanding and mitigating heat in urban areas*. London; Sterling, VA: Earthscan, 2008.

[14] H. Akbari, “Energy Saving Potentials and Air Quality Benefits of Urban Heat Island Mitigation”.
[15] Y. Yamashita, K. Sakamoto, H. Akiyoshi, M. Takahashi, T. Nagashima, and L. B. Zhou, “Ozone and temperature response of a chemistry climate model to the solar cycle and sea surface temperature,” *J. Geophys. Res.*, vol. 115, no. D3, p. 2009JD013436, Feb. 2010, doi: 10.1029/2009JD013436.
[16] B. J. Bloomer, J. W. Stehr, C. A. Piety, R. J. Salawitch, and R. R. Dickerson, “Observed relationships of ozone air pollution with temperature and emissions,” *Geophysical Research Letters*, vol. 36, no. 9, p. 2009GL037308, May 2009, doi: 10.1029/2009GL037308.
[17] M. Pomerantz, H. Akbari, L. B. Laboratory, and J. T. Harvey, “Cooler Reflective Pavements Give Benefits Beyond Energy Savings: Durability and Illumination”.
[18] Young, M., et al., “‘Field application of PCM in concrete pavement,’ Energy and Buildings, 2016, 122: 228-234.”.
[19] Wei, H., et al., “‘Phase change materials for thermal regulation of concrete,’ Journal of Cleaner Production, 2017, 162: 1182-1191.”.
[20] Lin, K.P., et al., “‘Experimental study on microencapsulated PCM for thermal management,’ Energy Conversion and Management, 2005, 46(6): 847-861.”.
[21] Y. Farnam, H. S. Esmaeeli, P. D. Zavattieri, J. Haddock, and J. Weiss, “Incorporating phase change materials in concrete pavement to melt snow and ice,” *Cement and Concrete Composites*, vol. 84, pp. 134–145, Nov. 2017, doi: 10.1016/j.cemconcomp.2017.09.002.
[22] D. P. Bentz and R. Turpin, “Potential applications of phase change materials in concrete technology,” *Cement and Concrete Composites*, vol. 29, no. 7, pp. 527–532, Aug. 2007, doi: 10.1016/j.cemconcomp.2007.04.007.
[23] Y. Farnam, A. Wiese, D. Bentz, J. Davis, and J. Weiss, “Damage development in cementitious materials exposed to magnesium chloride deicing salt,” *Construction and Building Materials*, vol. 93, pp. 384–392, Sep. 2015, doi: 10.1016/j.conbuildmat.2015.06.004.
[24] M. Hunger, A. G. Entrop, I. Mandilaras, H. J. H. Brouwers, and M. Founti, “The behavior of self-compacting concrete containing micro-encapsulated Phase Change Materials,” *Cement and Concrete Composites*, vol. 31, no. 10, pp. 731–743, Nov. 2009, doi: 10.1016/j.cemconcomp.2009.08.002.
[25] Ramakrishnan, S., et al.,. “Influence of phase change material (PCM) on the properties of concrete. Cement and Concrete Research, 96, 26-35,” 2017.
[26] Jayalath, A., et al.,. “Thermal properties of concrete with microencapsulated phase change materials. Journal of Materials in Civil Engineering, 28(7), 04016034,” 2016.
[27] U.S. Environmental Protection Agency. (2025). *What are heat islands?* Retrieved November 29, 2025, from https://www.epa.gov/heatislands/what-are-heat-islands epa.gov
[28] Gartland, L. (2008). *Heat islands: Understanding and mitigating heat in urban areas*. Earthscan.
[29] D. J. Sailor, “Opportunities and Challenges for Mitigation and Adaptation,” Toronto, 2002.

[30] Yamashita, Y., Sakamoto, K., Akiyoshi, H., Takahashi, M., Nagashima, T., & Zhou, L. B. (2010). Ozone and temperature response of a chemistry climate model to the solar cycle and sea surface temperature. *Journal of Geophysical Research: Atmospheres, 115*(D3), D031436. https://doi.org/10.1029/2009JD013436.
[31] M. Z. Chen, W. Wei, and S. P. Wu, "On Cold Materials of Pavement and High-Temperature Performance of Asphalt Concrete," *MSF*, vol. 620–622, pp. 379–382, Apr. 2009, doi: 10.4028/www.scientific.net/MSF.620-622.379.
[32] T. Nishizawa, T. Ozeki, K. Katoh, and K. Matsui, "Finite Element Model Analysis of Thermal Stresses of Thick Airport Concrete Pavement Slabs," *Transportation Research Record*, vol. 2095, no. 1, pp. 3–12, Jan. 2009, doi: 10.3141/2095-01.
[33] D. P. Johnston and R. W. Surdahl, "Influence of Mixture Design and Environmental Factors on Continuously Reinforced Concrete Pavement Cracking," *Transportation Research Record*, vol. 2020, no. 1, pp. 83–88, Jan. 2007, doi: 10.3141/2020-11.
[34] M. Santamouris, "Using cool pavements as a mitigation strategy to fight urban heat island—A review of the actual developments," *Renewable and Sustainable Energy Reviews*, vol. 26, pp. 224–240, Oct. 2013, doi: 10.1016/j.rser.2013.05.047.
[35] H. Li, J. T. Harvey, T. J. Holland, and M. Kayhanian, "The use of reflective and permeable pavements as a potential practice for heat island mitigation and stormwater management," *Environ. Res. Lett.*, vol. 8, no. 1, p. 015023, Mar. 2013, doi: 10.1088/1748-9326/8/1/015023.
[36] H. Akbari and H. D. Matthews, "Global cooling updates: Reflective roofs and pavements," *Energy and Buildings*, vol. 55, pp. 2–6, Dec. 2012, doi: 10.1016/j.enbuild.2012.02.055.
[37] M. Pomerantz, H. Akbari, P. Berdahl, S. J. Konopacki, H. Taha, and A. H. Rosenfeld, "Reflective surfaces for cooler buildings and cities," *Philosophical Magazine B*, vol. 79, no. 9, pp. 1457–1476, Sep. 1999, doi: 10.1080/13642819908216984.
[38] A. Synnefa, M. Santamouris, and K. Apostolakis, "On the development, optical properties and thermal performance of cool colored coatings for the urban environment," *Solar Energy*, vol. 81, no. 4, pp. 488–497, Apr. 2007, doi: 10.1016/j.solener.2006.08.005.
[39] L. Haselbach, M. Boyer, J. T. Kevern, and V. R. Schaefer, "Cyclic Heat Island Impacts on Traditional versus Pervious Concrete Pavement Systems," *Transportation Research Record*, vol. 2240, no. 1, pp. 107–115, Jan. 2011, doi: 10.3141/2240-14.
[40] J. T. Kevern and V. R. Schaefer, "Temperature Response in a Pervious Concrete System Designed for Stormwater Treatment," in *GeoCongress 2008*, New Orleans, Louisiana, United States: American Society of Civil Engineers, Mar. 2008, pp. 1137–1144. doi: 10.1061/40971(310)142.
[41] R. Mallick, J. Carelli, L. Albano, S. Bhowmick, and A. Veeraragavan, "Evaluation of the potential of harvesting heat energy from asphalt pavements," *International Journal of Sustainable Engineering*, vol. 4, no. 2, pp. 164–171, Jun. 2011, doi: 10.1080/19397038.2010.550336.
[42] R. B. Mallick, B.-L. Chen, and S. Bhowmick, "Harvesting energy from asphalt pavements and reducing the heat island effect," *International Journal of Sustainable Engineering*, vol. 2, no. 3, pp. 214–228, Sep. 2009, doi: 10.1080/19397030903121950.

[43] G. Wu and X. Yu, "System design to harvest thermal energy across pavement structure," in *2012 IEEE Energytech*, Cleveland, OH, USA: IEEE, May 2012, pp. 1–4. doi: 10.1109/EnergyTech.2012.6304703.
[44] H. Akbari, H. Damon Matthews, and D. Seto, "The long-term effect of increasing the albedo of urban areas," *Environ. Res. Lett.*, vol. 7, no. 2, p. 024004, Jun. 2012, doi: 10.1088/1748-9326/7/2/024004.
[45] S. Bretz, H. Akbari, and A. Rosenfeld, "Practical issues for using solar-reflective materials to mitigate urban heat islands," *Atmospheric Environment*, vol. 32, no. 1, pp. 95–101, Jan. 1998, doi: 10.1016/S1352-2310(97)00182-9.
[46] Y. Qin, "A review on the development of cool pavements to mitigate urban heat island effect," *Renewable and Sustainable Energy Reviews*, vol. 52, pp. 445–459, Dec. 2015, doi: 10.1016/j.rser.2015.07.177.
[47] M. Pomerantz, B. Ppn, and H. Akbari, "The Effect of Pavements' Temperatures on Air Temperatures in Large Cities".
[48] M. Pomerantz, H. Akbari, S.-C. Chang, R. Levinson, and B. Pon, "Examples of cooler reflective streets for urban heat-island mitigation: Portland cement concrete and chip seals," LBNL--49283, 816205, Apr. 2003. doi: 10.2172/816205.
[49] N. Tran, B. Powell, H. Marks, R. West, and A. Kvasnak, "Strategies for Design and Construction of High-Reflectance Asphalt Pavements," *Transportation Research Record*, vol. 2098, no. 1, pp. 124–130, Jan. 2009, doi: 10.3141/2098-13.
[50] R. Levinson, H. Akbari, P. Berdahl, K. Wood, W. Skilton, and J. Petersheim, "A novel technique for the production of cool colored concrete tile and asphalt shingle roofing products," *Solar Energy Materials and Solar Cells*, vol. 94, no. 6, pp. 946–954, Jun. 2010, doi: 10.1016/j.solmat.2009.12.012.
[51] R. Levinson, H. Akbari, and J. C. Reilly, "Cooler tile-roofed buildings with near-infrared-reflective non-white coatings," *Building and Environment*, vol. 42, no. 7, pp. 2591–2605, Jul. 2007, doi: 10.1016/j.buildenv.2006.06.005.
[52] R. Levinson, P. Berdahl, and H. Akbari, "Solar spectral optical properties of pigments—Part I: model for deriving scattering and absorption coefficients from transmittance and reflectance measurements," *Solar Energy Materials and Solar Cells*, vol. 89, no. 4, pp. 319–349, Dec. 2005, doi: 10.1016/j.solmat.2004.11.012.
[53] R. Levinson, P. Berdahl, and H. Akbari, "Solar spectral optical properties of pigments—Part II: survey of common colorants," *Solar Energy Materials and Solar Cells*, vol. 89, no. 4, pp. 351–389, Dec. 2005, doi: 10.1016/j.solmat.2004.11.013.
[54] A. Synnefa, M. Santamouris, and I. Livada, "A study of the thermal performance of reflective coatings for the urban environment," *Solar Energy*, vol. 80, no. 8, pp. 968–981, Aug. 2006, doi: 10.1016/j.solener.2005.08.005.
[55] M. L. Marceau and M. G. VanGeem, "Solar Reflectance Values for Concrete".
[56] R. Levinson and H. Akbari, "Effects of composition and exposure on the solar reflectance of portland cement concrete," *Cement and Concrete Research*, 2002.

[57] K. Boriboonsomsin and F. Reza, "Mix Design and Benefit Evaluation of High Solar Reflectance Concrete for Pavements," *Transportation Research Record*, vol. 2011, no. 1, pp. 11–20, Jan. 2007, doi: 10.3141/2011-02.
[58] J. W. Mack, L. D. Hawbaker, and L. W. Cole, "Ultrathin Whitetopping: State-of-the-Practice for Thin Concrete Overlays of Asphalt," *Transportation Research Record*, vol. 1610, no. 1, pp. 39–43, Jan. 1998, doi: 10.3141/1610-07.
[59] J. Mullaney and T. Lucke, "Practical Review of Pervious Pavement Designs," *CLEAN Soil Air Water*, vol. 42, no. 2, pp. 111–124, Feb. 2014, doi: 10.1002/clen.201300118.
[60] T. Asaeda and V. T. Ca, "Characteristics of permeable pavement during hot summer weather and impact on the thermal environment," *Building and Environment*, vol. 35, no. 4, pp. 363–375, May 2000, doi: 10.1016/S0360-1323(99)00020-7.
[61] C. T. Andersen, I. D. L. Foster, and C. J. Pratt, "The role of urban surfaces (permeable pavements) in regulating drainage and evaporation: development of a laboratory simulation experiment," *Hydrol. Process.*, vol. 13, no. 4, pp. 597–609, Mar. 1999, doi: 10.1002/(SICI)1099-1085(199903)13:4<597:AID-HYP756>3.0.CO;2-Q.
[62] J. Kevern, K. Wang, M. T. Suleiman, and V. R. Schaefer, "Mix Design Development for Pervious Concrete in Cold Weather Climates".
[63] R. M. Roseen *et al.*, "Seasonal Performance Variations for Storm-Water Management Systems in Cold Climate Conditions," *J. Environ. Eng.*, vol. 135, no. 3, pp. 128–137, Mar. 2009, doi: 10.1061/(ASCE)0733-9372(2009)135:3(128).
[64] J. T. Kevern, V. R. Schaefer, and K. Wang, "Temperature Behavior of Pervious Concrete Systems," *Transportation Research Record*, vol. 2098, no. 1, pp. 94–101, Jan. 2009, doi: 10.3141/2098-10.
[65] R. Zhang, G. Jiang, and J. Liang, "The Albedo of Pervious Cement Concrete Linearly Decreases with Porosity," *Advances in Materials Science and Engineering*, vol. 2015, pp. 1–5, 2015, doi: 10.1155/2015/746592.
[66] C. Syrrakou and G. F. Pinder, "Experimentally Determined Evaporation Rates in Pervious Concrete Systems," *J. Irrig. Drain Eng.*, vol. 140, no. 1, p. 04013003, Jan. 2014, doi: 10.1061/(ASCE)IR.1943-4774.0000652.
[67] E. M. Nemirovsky, A. L. Welker, and R. Lee, "Quantifying Evaporation from Pervious Concrete Systems: Methodology and Hydrologic Perspective," *J. Irrig. Drain Eng.*, vol. 139, no. 4, pp. 271–277, Apr. 2013, doi: 10.1061/(ASCE)IR.1943-4774.0000541.
[68] T. Nakayama and T. Fujita, "Cooling effect of water-holding pavements made of new materials on water and heat budgets in urban areas," *Landscape and Urban Planning*, vol. 96, no. 2, pp. 57–67, May 2010, doi: 10.1016/j.landurbplan.2010.02.003.
[69] H. Yamagata, M. Nasu, M. Yoshizawa, A. Miyamoto, and M. Minamiyama, "Heat Island mitigation using water retentive pavement sprinkled with reclaimed wastewater," *Water Science and Technology*, vol. 57, no. 5, pp. 763–771, Apr. 2008, doi: 10.2166/wst.2008.187.

[70] B. Zalba, J. M. Marín, L. F. Cabeza, and H. Mehling, "Review on thermal energy storage with phase change: materials, heat transfer analysis and applications," *Applied Thermal Engineering*, vol. 23, no. 3, pp. 251–283, Feb. 2003, doi: 10.1016/S1359-4311(02)00192-8.
[71] F. Fernandes *et al.*, "On the feasibility of using phase change materials (PCMs) to mitigate thermal cracking in cementitious materials," *Cement and Concrete Composites*, vol. 51, pp. 14–26, Aug. 2014, doi: 10.1016/j.cemconcomp.2014.03.003.
[72] Marani, A., & Nehdi, M. L. (2019). Integrating phase change materials in construction materials: Critical review. *Construction and Building Materials, 217*, 36–49. https://doi.org/10.1016/j.conbuildmat.2019.05.064
[73] A. Jamekhorshid, S. M. Sadrameli, and M. Farid, "A review of microencapsulation methods of phase change materials (PCMs) as a thermal energy storage (TES) medium," *Renewable and Sustainable Energy Reviews*, vol. 31, pp. 531–542, Mar. 2014, doi: 10.1016/j.rser.2013.12.033.
[74] H.-W. Min, S. Kim, and H. S. Kim, "Investigation on thermal and mechanical characteristics of concrete mixed with shape stabilized phase change material for mix design," *Construction and Building Materials*, vol. 149, pp. 749–762, Sep. 2017, doi: 10.1016/j.conbuildmat.2017.05.176.
[75] A. R. Sakulich and D. P. Bentz, "Incorporation of phase change materials in cementitious systems via fine lightweight aggregate," *Construction and Building Materials*, vol. 35, pp. 483–490, Oct. 2012, doi: 10.1016/j.conbuildmat.2012.04.042.
[76] S. A. Memon, H. Z. Cui, H. Zhang, and F. Xing, "Utilization of macro encapsulated phase change materials for the development of thermal energy storage and structural lightweight aggregate concrete," *Applied Energy*, vol. 139, pp. 43–55, Feb. 2015, doi: 10.1016/j.apenergy.2014.11.022.
[77] Y. Cai, G. Sun, M. Liu, J. Zhang, Q. Wang, and Q. Wei, "Fabrication and characterization of capric–lauric–palmitic acid/electrospun SiO2 nanofibers com`posite as form-stable phase change material for thermal energy storage/retrieval," *Solar Energy*, vol. 118, pp. 87–95, Aug. 2015, doi: 10.1016/j.solener.2015.04.042.
[78] B. A. Young, G. Falzone, Z. Wei, G. Sant, and L. Pilon, "Reduced-scale experiments to evaluate performance of composite building envelopes containing phase change materials," *Construction and Building Materials*, vol. 162, pp. 584–595, Feb. 2018, doi: 10.1016/j.conbuildmat.2017.11.160.
[79] Y. Han and J. E. Taylor, "Simulating the Inter-Building Effect on energy consumption from embedding phase change materials in building envelopes," *Sustainable Cities and Society*, vol. 27, pp. 287–295, Nov. 2016, doi: 10.1016/j.scs.2016.03.001.
[80] A. Marani and M. L. Nehdi, "Integrating phase change materials in construction materials: Critical review," *Construction and Building Materials*, vol. 217, pp. 36–49, Aug. 2019, doi: 10.1016/j.conbuildmat.2019.05.064.
[81] B. Ma, S. S. Wang, and J. Li, "Study on Application of PCM in Asphalt Mixture," *AMR*, vol. 168–170, pp. 2625–2630, Dec. 2010, doi: 10.4028/www.scientific.net/AMR.168-170.2625.

[82] B. Ma, J. Li, X. M. Wang, and N. Xiao, "Effect of Composite Shape-Stabilized Phase Change Material on Asphalt Mixture Temperature," *AMR*, vol. 311–313, pp. 2151–2154, Aug. 2011, doi: 10.4028/www.scientific.net/AMR.311-313.2151.
[83] B. Ma, W. Si, J. Ren, H. Wang, F. Liu, and J. Li, "Exploration of road temperature-adjustment material in asphalt mixture," *Road Materials and Pavement Design*, vol. 15, no. 3, pp. 659–673, Jul. 2014, doi: 10.1080/14680629.2014.885462.
[84] Meizhu Chen, Guangji Xu, Shaopeng Wu, and Shaoping Zheng, "High-temperature hazards and prevention measurements for asphalt pavement," in *2010 International Conference on Mechanic Automation and Control Engineering*, Wuhan, China: IEEE, Jun. 2010, pp. 1341–1344. doi: 10.1109/MACE.2010.5536275.
[85] M.Z. Chen,, L. Wan, and J.T. Lin, "Effect of Phase-Change Materials on Thermal and Mechanical Properties of Asphalt Mixtures.".
[86] B. Ma, S. Adhikari, Y. Chang, J. Ren, J. Liu, and Z. You, "Preparation of composite for highway pavements," *Construction and Building Materials*, vol. 42, pp. 114–121, May 2013, doi: 10.1016/j.conbuildmat.2012.12.027.
[87] Y. Farnam *et al.*, "Evaluating the Use of Phase Change Materials in Concrete Pavement to Melt Ice and Snow," *J. Mater. Civ. Eng.*, vol. 28, no. 4, p. 04015161, Apr. 2016, doi: 10.1061/(ASCE)MT.1943-5533.0001439.
[88] J. H. Yeon and K.-K. Kim, "Potential applications of phase change materials to mitigate freeze-thaw deteriorations in concrete pavement," *Construction and Building Materials*, vol. 177, pp. 202–209, Jul. 2018, doi: 10.1016/j.conbuildmat.2018.05.113.
[89] J. Skovajsa and M. Zalesak, "The Use of the Photovoltaic System in Combination with a
[90] Texas Department of Transportation. (2024). *Standard specifications for construction and maintenance of highways, streets, and bridges* (2024 Spec Book, September 1, 2024). https://www.txdot.gov/content/dam/docs/specifications/2024/spec-book-0924.pdf
[91] Radwan, I., & Dessouky, S. (2024). *Thermally Conductive Pre-cast Concrete Pavement for Urban Heat Island Mitigation* (Final Report UT-23-RP-01). Transportation Infrastructure Precast Innovation Center (TRANS-IPIC), University Transportation Center, University of Illinois Urbana-Champaign.

ACKNOWLEDGEMENTS

The authors gratefully acknowledge the support of the U.S. Department of Transportation (USDOT) and the Transportation Infrastructure Precast Innovation Center (TRANS-IPIC) at the University of Illinois Urbana–Champaign, whose funding and engagement were essential to this project. The City of San Antonio and the Texas Department of Transportation (TxDOT) are thanked for providing mix design guidance, testing procedures, and broader implementation context for concrete sidewalk applications. Ingram Ready Mix is acknowledged for supplying concrete materials consistent with local practice. The authors thank Microtek for providing the phase change materials and technical input on PCM use in precast systems, and Tindall Company and Capital Precast for their feedback on precast production and potential implementation pathways. Six Site Services is acknowledged as the contractor responsible for constructing the full-scale sidewalk test sections and for supporting field activities. Special thanks are extended to Dr. Alan Whittington for access to his laboratory, equipment, and guidance on thermal property measurements, and to Dr. Arturo Montoya for his contributions to the finite element modelling and interpretation of numerical results. Finally, the authors appreciate the assistance of students, staff, and technical personnel who contributed to specimen preparation, testing, instrumentation, and data collection.